Systems/Circuits

Novel Subunit-Specific Tonic GABA Currents and Differential Effects of Ethanol in the Central Amygdala of CRF Receptor-1 Reporter Mice

Melissa A. Herman,[1] Candice Contet,[1] Nicholas J. Justice,[3] Wylie Vale,[2†] and Marisa Roberto[1]

[1]Committee on the Neurobiology of Addictive Disorders, The Scripps Research Institute, La Jolla, California 92037, [2]Clayton Foundation Laboratories for Peptide Biology, The Salk Institute for Biological Studies, La Jolla, California 92037, and [3]Huffington Center on Aging, Baylor College of Medicine, Houston, Texas 77030

The central nucleus of the amygdala (CeA) is an important integrative site for the reinforcing effects of drugs of abuse, such as ethanol. Activation of corticotropin-releasing factor type 1 (CRF1) receptors in the CeA plays a critical role in the development of ethanol dependence, but these neurons remain uncharacterized. Using CRF1:GFP reporter mice and a combined electrophysiological/immunohistochemical approach, we found that CRF1 neurons exhibit an α1 $GABA_A$ receptor subunit-mediated tonic conductance that is driven by action potential-dependent GABA release. In contrast, unlabeled CeA neurons displayed a δ subunit-mediated tonic conductance that is enhanced by ethanol. Ethanol increased the firing discharge of CRF1 neurons and decreased the firing discharge of unlabeled CeA neurons. Retrograde tracing studies indicate that CeA CRF1 neurons project into the bed nucleus of the stria terminalis. Together, these data demonstrate subunit-specific tonic signaling and provide mechanistic insight into the specific effects of ethanol on CeA microcircuitry.

Introduction

The central amygdala (CeA) is primarily a GABAergic nucleus and a critical component of the neurocircuitry underlying the reinforcing effects of ethanol (EtOH) and drugs of abuse, known as the extended amygdala. The extended amygdala comprises the CeA, the bed nucleus of the stria terminalis (BNST), and the shell of the nucleus accumbens (Alheid and Heimer, 1988). Neuroplastic changes in GABAergic transmission in the CeA have been implicated in the transition from recreational use to alcohol dependence, or alcoholism (Hyyti ä and Koob, 1995; Roberts et al., 1996). We showed previously that GABAergic transmission is enhanced at presynaptic sites in the CeA after acute and chronic EtOH exposure (Roberto et al., 2003; Roberto et al., 2004). However, these studies focused solely on phasic inhibition. No studies have investigated the existence of tonic inhibitory signaling in the CeA and how it may be affected by EtOH. Because tonic inhibition plays a critical role in regulating network activity in other brain regions (Semyanov et al., 2004) and is a significant target of EtOH-induced neuroadaptation (Wallner et al., 2003; Liang et al., 2007; Mody et al., 2007; Pignataro et al., 2007; Liang et al., 2009; Nie et al., 2011), we hypothesized that tonic inhibition is present in CeA neurons and that EtOH alters this tonic inhibition to produce changes in network activity.

The actions of corticotropin releasing factor (CRF) at the CRF receptor-1 (CRF1) in the CeA have been implicated in the physiological responses to stress, as well as the development of alcohol dependence (Koob and Heinrichs, 1999; Koob, 2008, 2010). We showed previously that, like EtOH, CRF enhances GABA release in the CeA via actions at presynaptic CRF1 in rats and mice (Nie et al., 2004; Roberto et al., 2010). In addition, accumulating evidence implicates CRF signaling in the development and maintenance of alcohol dependence at both cellular (Merlo Pich et al., 1995; Roberto et al., 2010; Lowery-Gionta et al., 2012) and behavioral levels (Chu et al., 2007; Funk et al., 2007; Lowery et al., 2008; Roberto et al., 2010). These data demonstrate the significance of the CRF/CRF1 system in the CeA in all stages of alcohol dependence. However, because of technical limitations related to identifying specific neuronal populations, no study has directly examined CRF1-containing neurons in the CeA and their place in the larger circuitry of the extended amygdala. This limitation confounds the integration of cellular and behavioral data in determining the effects of EtOH within the extended amygdala.

Here, we used a bacterial artificial chromosome (BAC) transgenic mouse line expressing green fluorescent protein (GFP) in CRF1-containing neurons (Justice et al., 2008) and a combined electrophysiological and immunohistochemical approach to (1)

Received May 23, 2012; revised Dec. 6, 2012; accepted Dec. 8, 2012.

Author contributions: M.A.H., C.C., and M.R. designed research; M.A.H. performed research; N.J.J. and W.V. contributed unpublished reagents/analytic tools; M.A.H. and M.R. analyzed data; M.A.H., C.C., and M.R. wrote the paper.

This work was supported by the Pearson Center for Alcoholism and Addiction Research, the Clayton Medical Research Foundation, National Institute on Alcohol Abuse and Alcoholism Grants F32AA020430, AA020913, AA015566, AA06420, AA016985, and AA017447, and National Institute of Diabetes and Digestive and Kidney Diseases Grant P01DK026741. We thank Paul Schweitzer, George Siggins, and Floyd Bloom for their valuable comments. This is The Scripps Research Institute Manuscript 21762.

†Deceased, January 3, 2012.

The authors declare no competing financial interests.

Correspondence should be addressed to Dr. Melissa Herman, SP30-1150, 10550 North Torrey Pines Road, La Jolla, CA 92037. E-mail: mherman@scripps.edu.

DOI:10.1523/JNEUROSCI.2490-12.2013

 0270-6474/13/333284-15$15.00/0

characterize inhibitory transmission in CRF1 neurons in the CeA, (2) examine their place in local CeA microcircuitry, and (3) determine the effects of acute EtOH on the activity of this microcircuitry and downstream targets in the extended amygdala.

Materials and Methods

Brain slice preparation. All procedures were approved by The Scripps Research Institute Institutional Animal Care and Use Committee and were consistent with the National Institutes of Health *Guide for the Care and Use of Laboratory Animals.* We prepared slices from 57 transgenic adult male mice (2–6 months, 19–30 g) that express GFP under the control of the promoter of the CRF1 receptor gene (*Crhr1*). These mice were generated using BAC recombination techniques such that the first exon of *Crhr1* was replaced with the sequence encoding GFP. For a detailed description of the transgene design and immunohistochemical validation of these mice, see Justice et al. (2008).

Mice were subjected to brief anesthesia (3–5% isoflurane), followed by rapid decapitation and removal of the brain to an ice-cold high-sucrose solution, pH 7.3–7.4, that contained the following (in mM): 206.0 sucrose, 2.5 KCl, 0.5 $CaCl_2$, 7.0 $MgCl_2$, 1.2 NaH_2PO_4, 26 $NaHCO_3$, 5.0 glucose, and 5 HEPES. Brains were cut into transverse sections (300–400 μm) on a vibrating microtome (Leica VT1000S; Leica Microsystems) and placed in an oxygenated (95% O_2/5% CO_2) artificial CSF (aCSF) solution composed of the following (in mM): 120 NaCl, 2.5 KCl, 5 EGTA, 2.0 $CaCl_2$, 1.0 $MgCl_2$, 1.2 NaH_2PO_4, 26 $NaHCO_3$, 1.75 glucose, and 5 HEPES. Slices were incubated in this solution for 30 min at 35–37°C, followed by 30 min equilibration at room temperature (21–22°C). After equilibration, a single slice was transferred to a recording chamber mounted on the stage of an upright microscope (Olympus BX50WI).

Electrophysiological recording. We visualized neurons using infrared differential interference contrast (IR-DIC) optics and an EXi Aqua camera (QImaging). A 60× magnification water-immersion objective (Olympus) was used for identifying and approaching neurons. To avoid photolytic damage, initial exposure to episcopic fluorescence illumination was brief (<2 s). We detected fluorescent neurons using an X-Cite 120Q fluorescent illumination system (Lumen Dynamics) and captured images using QCapture software (QImaging). We made whole-cell (voltage-clamp and current-clamp) and juxtacellular (cell-attached) recordings with patch pipettes (4–6 MΩ; Warner Instruments) coupled to a Multiclamp 700B amplifier (Molecular Devices), low-pass filtered at 2–5 kHz, digitized (Digidata 1440A; Molecular Devices), and stored on a computer using pClamp 10 software (Molecular Devices). Series resistance was typically <10 MΩ and was continuously monitored with a hyperpolarizing 10 mV pulse. Electrophysiological properties of cells were determined by pClamp 10 Clampex software online during voltage-clamp recording using a 5 mV pulse delivered after breaking into the cell. The resting membrane potential was determined online after breaking into the cell using the zero current ($I = 0$) recording configuration, and the liquid junction potential was included in the determination.

The intracellular solution used for voltage- and current-clamp recordings was composed of the following (in mM): 145 KCl, 5 EGTA, 5 $MgCl_2$, 10 HEPES, 2 Na-ATP 2, and 0.2 Na-GTP. The pipette solution for juxtacellar (cell-attached) recordings was aCSF. Drugs were dissolved in aCSF and applied by either Y-tubing application for local perfusion primarily on the neuron of interest or bath perfusion. To isolate only the inhibitory currents mediated by $GABA_A$ receptors, recordings ($V_{hold} = -60$ mV) were performed in the presence of the glutamate receptor blockers 6,7-dinitroquinoxaline-2,3-dione (DNQX; 20 μM) and DL-2-amino-5-phosphonovalerate (AP-5; 50 μM) and the $GABA_B$ receptor antagonist CGP55845A [(2*S*)-3-[(15)-1-(3,4-dichlorophenyl)ethyl]amino-2-hydroxypropyl)(phenylmethyl)phosphinic acid] (CGP; 1 μM). All voltage-clamp and cell-attached recordings were performed in a gap-free acquisition mode with a sampling rate per signal of 10,000 Hz or a total data throughput equal of 20 kHz (2.29 MB/min). All current-clamp recordings were performed in sweeps with a sampling rate per signal of 10,000 Hz or a total data throughput equal of 20 kHz (2.29 MB/min) as defined by pClamp 10 Clampex software.

Paired recordings were performed using the same conditions described above and an intracellular solution composed of the following (in mM): 145 KCl, 5 EGTA (1 EGTA in low Ca^{2+} buffering conditions), 5 $MgCl_2$, 10 HEPES, 2 Na-ATP, and 0.2 Na-GTP. One cell (i.e., the "presynaptic" cell) was placed in current-clamp configuration and subjected to brief (10 ms) injections of current (400 pA) sufficient to produce one to two action potential spikes. The other cell (i.e., the "postsynaptic" cell) was placed in voltage-clamp configuration and held at −60 mV. Multiple sweeps (5–10) of current injection during simultaneous recordings were performed with a 10 s interval between sweeps. Dual recordings that displayed synaptic connectivity were superfused with DNQX, (20 μM), AP-5 (50 μM), and CGP (1 μM) to pharmacologically isolate $GABA_A$ receptor transmission. All paired (voltage- and current-clamp) recordings were performed in sweeps with a fast sampling rate of 10,000 Hz or a total data throughput of 40 kHz (4.58 MB/min) as defined by pClamp 10 Clampex software.

Immunohistochemistry. Adult male mice ($n = 4$) 2–5 months of age were deeply anesthetized by 35% chloral hydrate injection (0.4 ml, i.p.; Sigma), followed by transcardial perfusion with PBS and 4% paraformaldehyde (PFA). Brains were removed and stored in a cryoprotection solution (30% sucrose). After cryoprotection, brains were cut on a Cryocut1800 (Reichert Jung) into sequential 35 μm coronal sections, collected in PBS/0.1% Na-azide solution and stored at 4°C. We then incubated free-floating sections in a blocking solution (0.3% Triton X-100, 5% normal donkey serum, and 0.1% bovine serum albumin in PBS) for 1–2 h, followed by overnight incubation at 4°C in primary antibody diluted in 0.5% Tween 20 and 5% normal donkey serum in PBS. Primary antibodies used include anti-GFP (1:1000; Abcam) and anti-α1, anti-α5, anti-δ, and anti-γ2 $GABA_A$ receptor subunits (1:100; PhosphoSolutions). After washing, sections were transferred to a fluorophore-conjugated secondary antibody solution (Alexa Fluor 488 goat anti-chicken at 1:700, Invitrogen; or Cy3 donkey anti-rabbit at 1:200, Jackson ImmunoResearch) for 1–2 h at room temperature. After washing, the sections were mounted and coverslipped with Vectashield (Vector Laboratories). Slices were examined for immunofluorescence, and images of labeled neurons were digitally captured using a confocal microscope (Bio-Rad LaserSharp 2000 with emission wavelengths 488, 568, and 647 nm). Immunofluorescence was quantified using stereological principles to examine 10 randomly selected sections of CeA at 60× magnification from four mice.

Biocytin staining. In some cases, the intracellular solution for electrophysiological recordings included 3–5% (w/v) EZ-Link Biocytin (Thermo Fisher Scientific). We performed recordings as described above. After recording, we placed slices in 4% PFA and fixed overnight. Subsequent to fixation, we permeabilized slices in a 2% Triton X-100/PBS solution for 45 min and incubated in Avidin-D Texas Red (1:100; Vector Laboratories) in a 0.5% Triton X-100/PBS solution for 1.5–2 h. Slices were then washed repeatedly in PBS, mounted, and coverslipped with Vectashield (Vector Laboratories). Fluorescence was then detected and imaged on a confocal microscope (Bio-Rad LaserSharp 2000 with emission wavelengths 488, 568, and 647 nm).

Retrograde labeling of CeA neurons. Adult male mice ($n = 10$) 3–4 months of age were anesthetized with a 1–3% isoflurane/oxygen mixture, placed on a warming pad, and mounted in a stereotaxic frame (David Kopf Instruments). A vertical incision was made in the skin overlaying the skull, which was subsequently exposed and cleaned. Head placement was adjusted to a level skull position according to bregma and lambda coordinates. A small hole was drilled over the target brain site [dorsolateral BNST (dlBNST): 0.0 mm anteroposterior, ±1.1 mm mediolateral, −4.3 mm dorsoventral] based on the atlas of Franklin and Paxinos (2008). Bilateral 30 gauge stainless steel injector needles connected to Tygon tubing preloaded with fluorescent microspheres (530/590 nm excitation/emission; Lumafluor) were lowered to the dlBNST. We injected a volume of ~100 nl of undiluted fluorescent microspheres suspension over a 1–2 min period using a Hamilton microsyringe controlled by a pump (Harvard Apparatus). The injector needles were left in place for an additional 10 min to minimize backflow up the needle track. After withdrawal of the injector needles, the incision was closed and mice were allowed to recover from anesthesia. Mice were killed 1 week later by either 35% chloral hydrate injection (0.4 ml, i.p.) followed by processing for immunohistochemistry as described above ($n = 4$) or 3–5% isoflu-

rane followed by processing for electrophysiological recording as described above ($n = 6$).

Drugs and chemicals. We purchased DNQX (10 μM), AP-5 (50 μM), and CGP (1 μM) from Tocris Bioscience. We purchased bicuculline methiodide (60 μM), SR-95531 [2-(3-carboxypropyl)-3-amino-6-(4-methoxyphenyl)pyridazinium bromide] [gabazine (GBZ); 100 μM], strychnine (1 μM), 4,5,6,7-tetrahydroisoxazolo[5,4-c]pyridin-3-ol (THIP; 1–10 μM), tetrodotoxin (TTX; 1 μM), zolpidem (100 nM), and L655,708 (5 μM) from Sigma.

Statistical analyses. Frequency, amplitude, and decay of IPSCs were analyzed and visually confirmed using a semiautomated threshold-based mini-detection software (Mini Analysis; Synaptosoft). We determined averages of IPSC characteristics from baseline and experimental drug conditions containing a minimum of 60 events (time period of analysis varied as a product of individual event frequency), and we determined decay kinetics using exponential curve fittings and reported as decay time (milliseconds). All detected events were used for event frequency analysis, but superimposed events were eliminated for amplitude and decay kinetic analysis. In voltage-clamp recordings, we determined tonic currents using Clampfit 10.2 (Molecular Devices) and a previously described method (Glykys and Mody, 2007b) in which the mean holding current (i.e., the current required to maintain the −60 mV membrane potential) was obtained by a Gaussian fit to an all-points histogram over a 5 s interval. The all-points histogram was constrained to eliminate the contribution of IPSCs to the holding current. We quantified responses as the difference in holding current between baseline and experimental conditions. The frequency of firing discharge in cell-attached recordings was evaluated using threshold-based event detection analysis in Clampfit 10.2 (Molecular Devices). Events were analyzed for independent significance using a one-sample *t* test and compared using a two-tailed *t* test for independent samples, a paired two-tailed *t* test for comparisons made within the same recording, and a one-way ANOVA with a Bonferroni's *post hoc* analysis for comparisons made between three or more groups. All statistical analysis was performed using Prism 5.02 (GraphPad Software). Analysis of synaptic coupling was performed according to a previously described method (Debanne et al., 2008) with the criteria for synaptic coupling of a presynaptic action potential and a postsynaptic current consisting of a short delay (1–5 ms) with little variability in delay between sweeps. Data are presented as mean ± SE. In all cases, $p < 0.05$ was the criterion for statistical significance.

Results

Identification and characterization of CRF1 neurons in the CeA

GFP positive (GFP^+) CRF1-containing (CRF1) neurons were identified and differentiated from unlabeled (GFP^-) CeA neurons using fluorescent optics and brief (<2 s) episcopic illumination in slices from CRF1:GFP reporter mice. For the purpose of clarity, we refer to GFP^+ CRF1 neurons throughout as $CRF1^+$ and GFP^- neurons throughout as $CRF1^-$. During live-slice recording conditions, we typically observed individual $CRF1^+$ neurons in the medial portion of the CeA and therefore targeted neurons ($CRF1^+$ and $CRF1^-$) in this region. Consistent with the visualization of direct fluorescence during functional studies, immunohistochemical analysis of GFP expression confirmed that $CRF1^+$ neurons were located primarily in the medial portion of the CeA. A coronal section of the CeA with representative sites of $CRF1^+$ neurons (*) detected during live-slice recording is shown in Figure 1*A*. A $CRF1^+$ CeA neuron visualized using fluorescent optics (left) and IR-DIC optics (right) is shown in Figure 1*B*. GFP^+ expression in the CeA as detected using immunohistochemistry is shown in Figure 1*C*.

We used whole-cell current-clamp recordings and a step protocol consisting of hyperpolarizing to depolarizing current injections to determine the cell type of CeA neurons by spiking characteristics. As described previously (Dumont et al., 2002; Chieng et al., 2006), CeA neurons are composed of three principal cell types: (1) low-threshold bursting, which exhibit one or two action potentials elicited by depolarizing current steps and afterhyperpolarization action potentials; (2) late spiking, which exhibit delayed action potentials elicited by depolarizing current steps; and (3) regular spiking, which exhibit regular action potentials in response to depolarizing current steps. The majority (55 of 72, 76%) of $CRF1^+$ neurons were of the low-threshold bursting type (Fig. 1*D*, top), and a smaller proportion (17 of 72) were of the regular spiking type (Fig. 1*D*, bottom). $CRF1^-$ neurons were divided into the late spiking type (34 of 59, 58%; Fig. 1*D*, middle) and the regular spiking type (25 of 59, 42%; Fig. 1*D*, bottom). Importantly, we never observed any late spiking $CRF1^+$ neurons or low-threshold bursting $CRF1^-$ neurons, suggesting that these groups are mutually exclusive.

Phasic inhibitory transmission in $CRF1^+$ and $CRF1^-$ CeA neurons

We assessed baseline phasic $GABA_A$ receptor activity using whole-cell voltage-clamp recordings of spontaneous IPSCs (sIPSCs). $CRF1^+$ neurons had a significantly higher average baseline sIPSC frequency (6.1 ± 0.9 Hz; $n = 43$ from 15 mice) compared with $CRF1^-$ neurons (3.3 ± 0.5 Hz; $p < 0.05$; $n = 23$ from 10 mice) and no difference in sIPSC amplitude, rise time, or decay between $CRF1^+$ and $CRF1^-$ CeA neurons (Fig. 1*E*). $CRF1^+$ neurons possessed a significantly smaller membrane capacitance (C_m), lower time constant (tau), and higher resting membrane potential (V_m) than $CRF1^-$ neurons (Fig. 1*F*). Morphological analysis of $CRF1^+$ neurons found that they had an oval soma (~20–25 μm), projections that radiated out along the dorsoventral axis, and possessed a spiny dendritic morphology (Fig. 1*G*).

Tonic inhibitory transmission in $CRF1^+$ and $CRF1^-$ CeA neurons

After examining the phasic $GABA_A$ receptor activity in $CRF1^+$ neurons compared with $CRF1^-$ neurons, we assessed the tonic conductance in these two populations using whole-cell voltage-clamp recordings. A $GABA_A$ receptor-mediated tonic current was defined as the difference in holding current (i.e., the current required to maintain the neuron at −60 mV) before and after application of a $GABA_A$ receptor antagonist. Superfusion of the $GABA_A$ receptor antagonist GBZ (100 μM) produced a significant reduction in holding current in $CRF1^+$ neurons (19.7 ± 2.4 pA, $p < 0.05$, $n = 10$; Fig. 2*A*, top trace, *B*) that was not augmented by subsequent superfusion of 100 μM of the $GABA_A$ receptor channel blocker picrotoxin (PTX) (0.08 ± 1.6 pA, $n = 5$; Fig. 2*A*, top trace, *B*). Superfusion of PTX (100 μM) produced a reduction in holding current in $CRF1^+$ neurons that was not significantly different from that produced by GBZ (19.0 ± 3.1 pA, $p < 0.05$, $n = 9$; Fig. 2*A*, bottom trace, *B*) and not further augmented by subsequent application of GBZ (−0.6 ± 1.9 pA, $n = 5$; Fig. 2*A*, bottom trace, *B*). These data suggest that $CRF1^+$ neurons in the CeA possess an ongoing tonic $GABA_A$ receptor conductance and that spontaneous channel activity does not contribute to this tonic conductance.

Superfusion of GBZ (100 μM) produced no change in holding current in $CRF1^-$ neurons (−1.8 ± 2.7 pA, $n = 7$; Fig. 2*C*, top trace, *D*). However, superfusion of the GABA reuptake inhibitor nipecotic acid (1 mM) produced a significant increase in baseline holding current (68.4 ± 7.3 pA, $p < 0.05$, $n = 6$) and no significant change in frequency (86.7 ± 8.1% of control) or amplitude (97.2 ± 9.6% of control) of sIPSCs. Subsequent application of GBZ produced a significant reduction in holding current (56.4 ± 8.1 pA, $p < 0.05$, $n = 6$; Fig. 2*C*, bottom trace, *D*). These data

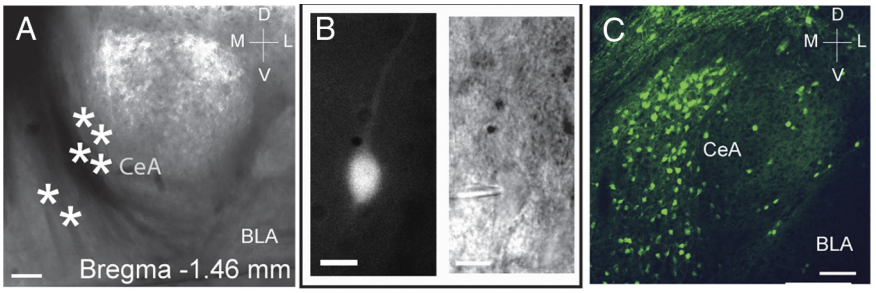

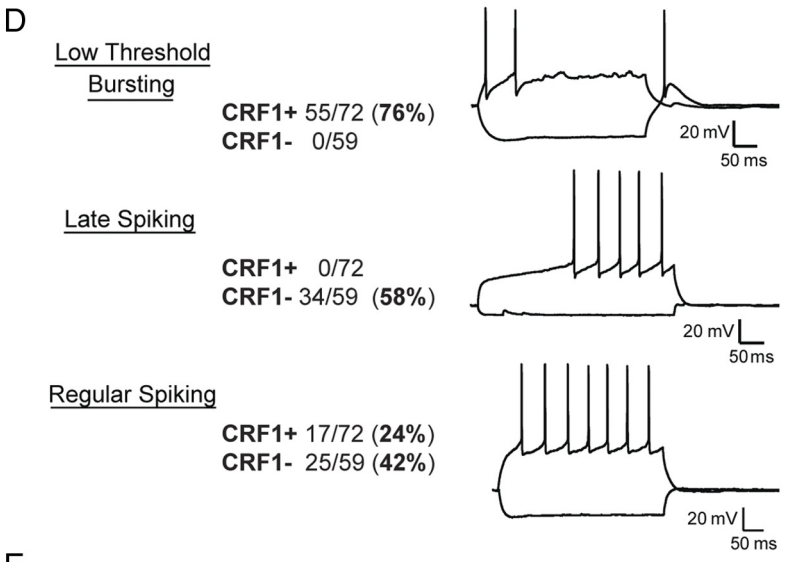

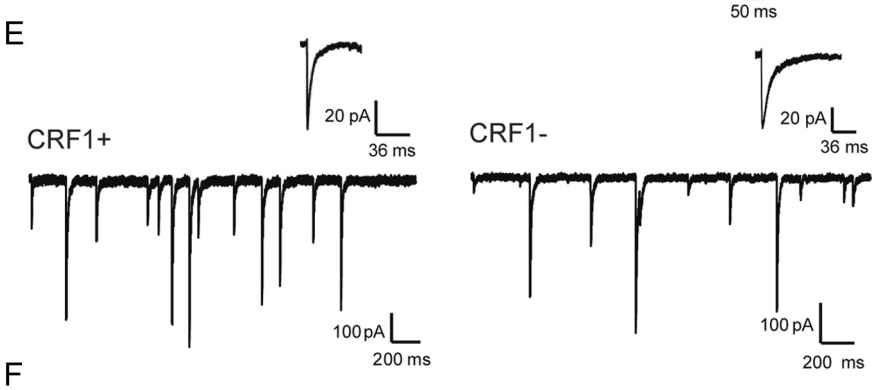

F

CeA neuron	Membrane Capacitance Cm (pF)	Membrane Resistance Rm (MΩ)	Time Constant Tau (ms)	Membrane Potential Vm (mV)
CRF1+	33.1 ± 1.5*	241.2 ± 16.4	334.6 ± 27.6*	-51.4 ± 2.4*
CRF1-	67.4 ± 3.6	241.9 ± 20.2	666.8 ± 46.0	-61.0 ± 1.4

*p<0.05 as compared to CRF1-

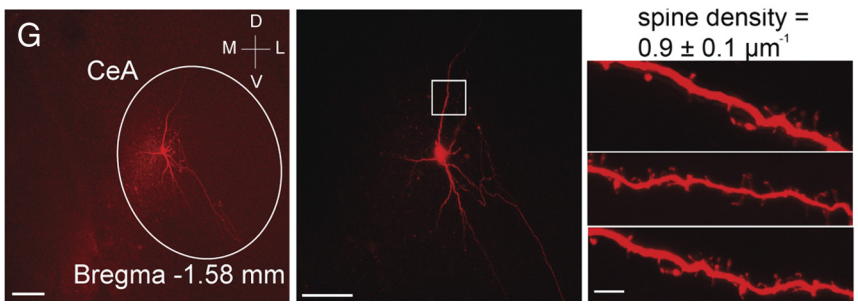

Figure 1. ***A***, A 10× magnification photomicrograph of a coronal CeA slice indicating recording sites of CRF1$^+$ neurons (*) and anatomical location (bregma −1.46 mm). Scale bar, 100 μm. ***B***, A 60× magnification of a CRF1$^+$ CeA neuron using fluorescent optics (left) and IR-DIC optics (right). Scale bar, 20 μm. ***C***, A 25× magnification photomicrograph of a coronal CeA slice illustrating GFP expression in the CeA of a CRF1:GFP reporter mouse. Scale bar, 50 μm. ***D***, Representative current-clamp recording illustrating spike characteristics of a low-threshold bursting CeA neuron (top trace), a late-spiking CeA neuron (middle trace), and a regular spiking CeA neuron (bottom trace) and the proportion of CRF1$^+$ and CRF1$^-$ neurons in each cell type. ***E***, Representative voltage-clamp recording of sIPSCs and scaled average sIPSC (inset) from a CRF1$^+$ neuron (top trace) and a CRF1$^-$ neuron (bottom trace). ***F***, Summary of membrane characteristics; *$p < 0.05$ comparing CRF1$^+$ to CRF1$^-$ by unpaired *t* test, $n = 27$ (CRF1$^+$) and $n = 21$ (CRF1$^-$). ***G***, A biocytin-filled CRF1$^+$ CeA neuron at 10× magnification (left), 25× magnification (middle), and a 60× magnification showing the primary dendrite indicated by the white box in the middle (right). Scale bars: left, 100 μm; middle, 50 μm; right, 5 μm. D, Dorsal; L, lateral; M, medial; V, ventral.

suggest that CRF1$^-$ neurons in the CeA do not possess an ongoing tonic conductance but have the potential for a tonic conductance that is evident when the local GABA concentration is elevated.

We also examined the possibility of a glycine receptor-mediated tonic conductance in the CeA, because this form of tonic conductance has been shown in the spinal cord (Mitchell et al., 2007) and may be important in other brain areas. Superfusion of the glycine receptor antagonist strychnine (1 μM) produced no change in holding current in either CRF1$^+$ or CRF1$^-$ neurons (−0.8 ± 2.2 pA, $n = 6$; 0.7 ± 3.5 pA, $n = 5$, respectively). In addition, strychnine produced no significant change in frequency or amplitude of sIPSCs in either CRF1$^+$ or CRF1$^-$ neurons. These data suggest that there is no ongoing glycine receptor-mediated tonic conductance in any of the CeA neurons that we studied.

To assess the impact of spontaneous phasic $GABA_A$ receptor transmission on the tonic conductance in CRF1$^+$ neurons in the CeA, we applied the Na^+ channel blocker TTX to block all action potential-mediated neurotransmission. Superfusion of TTX (1 μM) produced a significant reduction in holding current (25.6 ± 5.9 pA, $p < 0.05$, $n = 17$; Fig. 3*A*, top trace, *B*) and a significant reduction in IPSC frequency (55.2 ± 5.2% of control, $p < 0.05$, $n = 17$; Fig. 3*A*, top trace, *C*) in CRF1$^+$ neurons. In contrast, there was no change in holding current (−1.7 ± 1.1 pA, $n = 10$; Fig. 3*A*, bottom trace, *B*) or IPSC frequency (94.8 ± 8.7% of control, $n = 10$; Fig. 3*A*, bottom trace, *B*) in CRF1$^-$ neurons. The magnitude of the decrease in IPSC frequency in CRF1$^+$ neurons was positively correlated with the magnitude of the tonic current (slope = 9.0 ± 2.8, intercept = 5.1 ± 8.2, $R^2 = 0.43$, $p < 0.05$,

$n = 16$; Fig. 3*C*). The reduction in holding current produced by TTX was not significantly different from that produced by GBZ, and superfusion of TTX prevented the reduction in holding current observed with GBZ (1.6 ± 1.0 pA, $n = 7$; Fig. 3*D*). Collectively, these data suggest that the source of tonic conductance in CRF1$^+$ neurons in the CeA is action-potential-dependent GABA release.

Tonic $GABA_A$ receptor subunits in the CeA

Tonic $GABA_A$ receptors have a distinct subunit composition that confers the properties required to possess a tonic conductance (for review, see Glykys and Mody, 2007a). To assess the subunit composition of the $GABA_A$ receptors responsible for tonic conductance in the CeA, we used a combined pharmacological and immunohistochemical approach. The α4 or α6 subunit commonly associates with the δ subunit (Jones et al., 1997; Sur et al., 1999), and this receptor composition is associated with tonic conductance in a number of brain areas, including the hippocampus (Stell et al., 2003), cerebellum (Saxena and Macdonald, 1996), and cortex (Krook-Magnuson and Huntsman, 2005), so we first assessed the role of the δ subunit in the CeA. Focal application of the δ subunit-preferring agonist gaboxadol (THIP) to CRF1$^+$ neurons did not change holding current at concentrations ≤2 μM (Fig. 4*A*, top trace, *C*) and only altered holding current at concentrations ≥5 μM (16.8 ± 3.8 pA, $p < 0.05$, $n = 8$; Fig. 4*A*, bottom trace, *C*). In contrast, focal application of 2 μM THIP to CRF1$^-$ neurons significantly increased holding current (23.8 ± 6.7 pA, $p < 0.05$; $n = 5$; Fig. 4*B*, top trace, *C*), as did focal application of 5 μM THIP (82.6 ± 16.5 pA, $p < 0.05$; $n = 5$; Fig. 4*B*, bottom trace, *C*). The increase in holding current observed with 5 μM THIP in CRF1$^-$ neurons was not prevented by previous superfusion of TTX (25.0 ± 4.4 pA, $p < 0.05$, $n = 6$) but was blocked by previous superfusion of GBZ (0.7 ± 1.2 pA, $n = 6$), suggesting that the effects of THIP in CRF1$^-$ neurons are mediated by the $GABA_A$ receptor and are independent of action-potential-dependent GABA release. Although both CRF1$^+$ and CRF1$^-$ neurons displayed dose-dependent increases in holding current in response to THIP application, CRF1$^-$ neurons showed a significantly greater effect of THIP at all doses tested (Fig. 4*C*), suggesting that tonic signaling in CRF1$^-$ neurons is mediated by $GABA_A$ receptors that contain the δ subunit.

EtOH has been shown to augment tonic conductance in other brain regions (Carta et al., 2004; Hanchar et al., 2005; Jia et al., 2008), and the δ subunit has been implicated in this effect (Wei et al., 2004; Glykys et al., 2007). Focal application of EtOH (44 mM) for 20–30 s did not significantly change holding current in CRF1$^+$ neurons (4.6 ± 1.2 pA, $n = 5$; Fig. 4*D*, left trace, *E*) but did significantly increase holding current in CRF1$^-$ neurons (9.5 ± 1.7 pA, $p < 0.05$, $n = 5$; Fig. 4*D*, right trace, *E*). The increase in holding current observed with EtOH in CRF1$^-$ neurons was significantly augmented after previous superfusion of TTX (25.3 ± 5.1 pA, $p < 0.05$, $n = 7$), suggesting that the effects of EtOH are partially occluded by action-potential-dependent GABA release in the basal state. The increase in holding current observed with EtOH in CRF1$^-$ neurons was, however, blocked by previous superfusion of GBZ (−1.1 ± 1.0 pA, $n = 5$), suggesting that the effects of EtOH in CRF1$^-$ neurons are mediated by actions at the $GABA_A$ receptor. The effect of EtOH on spontaneous phasic transmission was assessed with a more prolonged superfusion of EtOH (3–5 min) to ensure an adequate sample size of sIPSCs for analysis. Superfusion of EtOH (44 mM) did not change sIPSC frequency in the majority of CRF1$^+$ neurons (93.6 ± 7.0% of control, $n = 8$; Fig. 4*F*). It should be noted that, in one neuron, a marked increase in sIPSC frequency was ob-

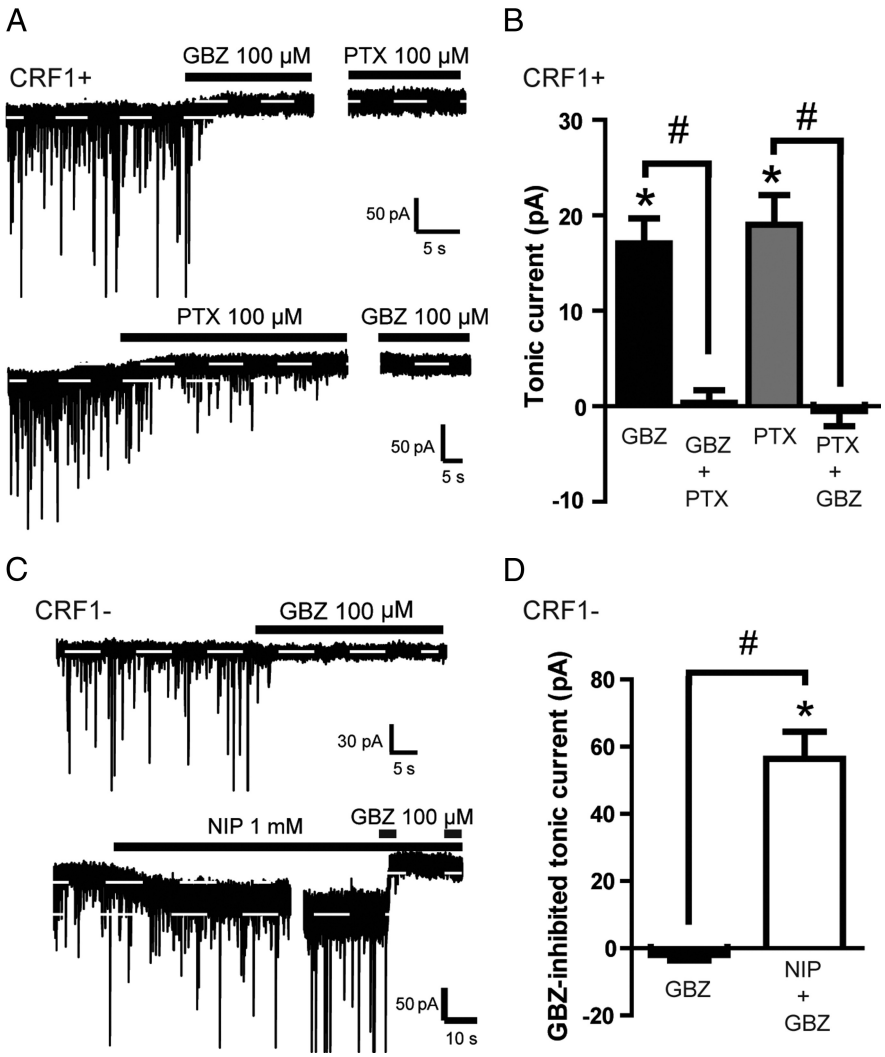

Figure 2. ***A***, Representative voltage-clamp recordings from a CRF1$^+$ neuron during superfusion of GBZ (100 μM), followed by PTX (100 μM, top trace) and during superfusion of PTX followed by GBZ (bottom trace). Dashed lines indicate average holding current. ***B***, Summary of the tonic current in CRF1$^+$ neurons revealed by superfusion of GBZ ($n = 10$) and PTX ($n = 9$) and occlusion of tonic current by previous superfusion of either GBZ ($n = 5$) or PTX ($n = 5$); $^*p < 0.05$ by one-sample *t* test, $^\#p < 0.05$ by unpaired *t* test. ***C***, Representative voltage-clamp recordings from a CRF1$^-$ neuron during superfusion of GBZ (100 μM, top trace) and during superfusion of nipecotic acid (NIP, 1 mM) followed by GBZ (bottom trace). Dashed lines indicate average holding current. ***D***, Summary of the tonic current in CRF1$^-$ neurons revealed by superfusion of GBZ alone ($n = 7$) and by superfusion of GBZ in the presence of NIP ($n = 6$). $^*p < 0.05$ by one-sample *t* test, $^\#p < 0.05$ by unpaired *t* test.

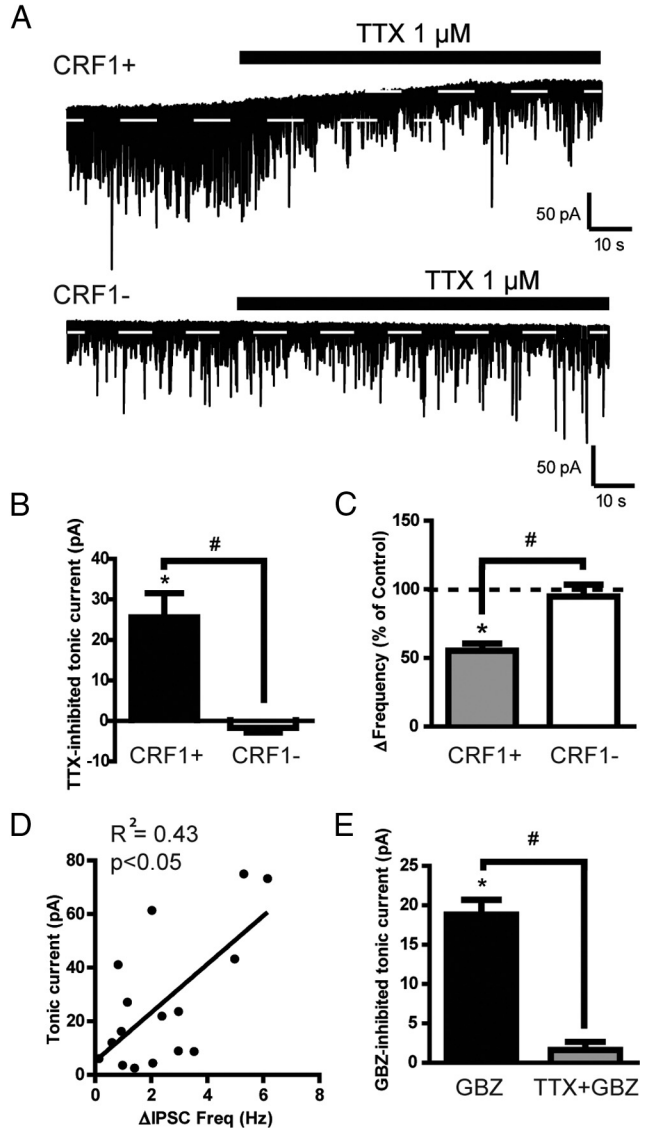

Figure 3. ***A***, Representative voltage-clamp recordings from a CRF1$^+$ neuron (top trace) and a CRF1$^-$ neuron (bottom trace) during superfusion of TTX (1 μM). Dashed lines indicate average holding current. ***B***, Summary of the tonic current revealed by TTX superfusion in CRF1$^+$ neurons ($n = 17$) and CRF1$^-$ neurons ($n = 10$); $^*p < 0.05$ by one-sample *t* test, $^\#p < 0.05$ by unpaired *t* test. ***C***, Summary of the change in IPSC frequency (% of Control) in CRF1$^+$ neurons ($n = 17$) and CRF1$^-$ neurons ($n = 10$); $^*p < 0.05$ by unpaired *t* test, $^\#p < 0.05$ by unpaired *t* test. ***D***, Summary of the correlation between the change in IPSC frequency and the magnitude of tonic current after TTX superfusion in CRF1$^+$ neurons; slope = 9.0 ± 2.8, intercept = 5.1 ± 8.2, $R^2 = 0.4329$, $p < 0.05$, $n = 16$. ***E***, Summary of the tonic current in CRF1$^+$ neurons revealed by GBZ superfusion alone and compared with GBZ after TTX superfusion ($n = 7$); $^*p <$ 0.05 by one-sample *t* test, $^\#p < 0.05$ by unpaired *t* test.

served, but this neuron was determined to be a statistical outlier and excluded from the analysis. In contrast, superfusion of EtOH (44 mM) significantly increased sIPSC frequency in all CRF1$^-$ neurons (138. 8 ± 11.7% of control, $p < 0.05$, $n = 6$; Fig. 4*F*). Superfusion of EtOH did not alter sIPSC amplitude or decay in either CRF1$^+$ or CRF1$^-$ neurons.

Based on the electrophysiological studies, we hypothesized that the δ subunit is expressed in the CeA and that it is primarily expressed in CRF1$^-$ neurons. Examination of 10 CeA sections at 60× magnification from four mice identified a total of 119 neurons that contained the CRF1 receptor (Fig. 4*G*, thick arrow), a total of 112 neurons that contained the δ subunit (Fig. 4*H*, thin arrow), and a total of 27 neurons that contained both the CRF1 receptor and the δ subunit (Fig. 4*I*, inset). Consistent with our functional studies, the immunohistochemical analysis confirmed that the δ subunit of the $GABA_A$ receptor is expressed in the CeA, primarily in CRF1$^-$ and not CRF1$^+$ CeA neurons. However, it should be noted that 23% of the CRF1$^+$ neurons examined did express the δ subunit, suggesting that there may be a specific subpopulation of CRF1$^+$ neurons in the CeA that do express the δ subunit.

Because the δ subunit did not appear to mediate the tonic conductance in CRF1$^+$ neurons, we assessed the contribution of other $GABA_A$ receptor subunits. The α5 subunit has been implicated in tonic currents in other brain areas, such as the hippocampus (Caraiscos et al., 2004; Scimemi et al., 2005; Glykys et al., 2008) and striatum (Ade et al., 2008), and is expressed in the CeA (Pirker et al., 2000). Thus, we examined whether the α5 subunit mediates the tonic conductance observed in CRF1$^+$ neurons using the inverse agonist L655–708 that, at low concentrations, preferentially acts at $GABA_A$ receptors containing the α5 subunit (Caraiscos et al., 2004). Focal application of L655,708 (5 μM) did not significantly affect the holding current in either CRF1$^+$ neurons (0.05 ± 1.7 pA, $n = 7$) or CRF1$^-$ neurons (2.1 ± 1.7 pA, $n = 5$). In addition, consistent with previous reports (Caraiscos et al., 2004), focal application of L655,798 did not significantly change the frequency, amplitude, or decay of sIPSCs in either CRF1$^+$ neurons or CRF1$^-$ neurons. These data suggest that the α5 subunit does not mediate tonic currents in any of the CRF1$^+$ or CRF1$^-$ CeA neurons studied.

We performed double-label immunohistochemical studies examining α5 subunit expression in the CRF1$^+$ and CRF1$^-$ neurons in the CeA. Examination of 10 CeA sections at 60× magnification identified 118 neurons that contained the CRF1 receptor, 122 neurons that contained the α5 subunit, and 24 neurons (20%) that contained both the CRF1 receptor and the α5 subunit. Our electrophysiological studies found no significant role for the α5 subunit in either CRF1$^+$ or CRF1$^-$ CeA neurons, but immunohistochemical analysis confirms that the α5 subunit is expressed in the CeA (Pirker et al., 2000), predominantly in CRF1$^-$ neurons. It is unclear whether the α5 subunit was expressed in a neuronal population not included in the experimental sample or whether the α5 subunit is not functionally expressed on the cell surface. Future studies will be required to elucidate the role of the α5 subunit in the CeA.

Because CRF1$^+$ neurons had a significantly higher baseline sIPSC frequency and possessed a TTX-sensitive tonic conductance, we hypothesized that the tonic $GABA_A$ receptors in CRF1$^+$ neurons are located in or near the synapse and that they contain the α1 subunit. To test this hypothesis, we used the benzodiazepine agonist zolpidem, which at low concentrations preferentially acts at $GABA_A$ receptors containing the α1 subunit (Sanger et al., 1996). Superfusion of zolpidem (100 nM) onto CRF1$^+$ neurons significantly increased holding current (20.9 ± 4.3 pA, $p < 0.05$, $n = 6$; Fig. 5*A*, top trace, *B*) that was reversed by subsequent superfusion of the $GABA_A$ receptor antagonist bicuculline (60 μM; 23.6 ± 6.0 pA, $p < 0.05$, $n = 6$; Fig. 5*A*, top trace, *C*). Superfusion of zolpidem had no significant effect on sIPSC frequency, amplitude, or rise time but did significantly increase decay from 3.5 ± 0.1 to 4.1 ± 0.2 ms ($p < 0.05$, $n = 6$). In contrast, superfusion of zolpidem (100 nM) onto CRF1$^-$ neurons did not significantly change holding current (3.7 ± 2.8 pA, $n = 6$; Fig. 5*A*, bottom trace, *B*) and only elicited a small decrease in holding current with subsequent superfusion of bicuculline (5.9 ± 1.7 pA, $n = 6$; Fig. 5*A*, bottom trace, *C*). Superfusion of

zolpidem did not change sIPSC frequency, amplitude, rise time, or decay in CRF1$^-$ neurons.

Based on the electrophysiological data, we hypothesized that the α1 subunit of the $GABA_A$ receptor was expressed primarily in CRF1$^+$ CeA neurons. Examination of 10 CeA sections at 60× magnification from four mice identified 121 neurons that contained the CRF1 receptor (Fig. 5*D*, top and middle arrow), 111 neurons that contained the α1 subunit (Fig. 5*E*, top and bottom arrows), and 94 neurons that contained both the CRF1 receptor and the α1 subunit (Fig. 4*F*, arrow). Consistent with the functional data, the α1 $GABA_A$ receptor subunit was expressed in the CeA and was expressed in the majority (78%) of CRF1$^+$ neurons. However, it is important to note that α1 expression was not observed in 22% of the CRF1$^+$ neurons examined and that some CeA neurons that expressed the α1 subunit were not CRF1$^+$, suggesting that a subpopulation of CRF1$^+$ neurons does not contain the α1 subunit and a subpopulation of CRF1$^-$ neurons does contain the α1 subunit.

We also performed double-label immunohistochemical experiments examining γ subunit expression in CRF1$^+$ and CRF1$^-$ neurons in the CeA. Examination of 10 CeA sections at 60× magnification from four mice identified 142 neurons that contained the CRF1 receptor, 165 neurons that contained the γ2 subunit, and 138 neurons (97%) that contained both the CRF1 receptor and the γ2 subunit. Consistent with previous reports (Pirker et al., 2000), the γ2 $GABA_A$ receptor subunit was expressed in the CeA and was expressed in both CRF1$^+$ and CRF1$^-$ neurons in an approximately equivalent proportion.

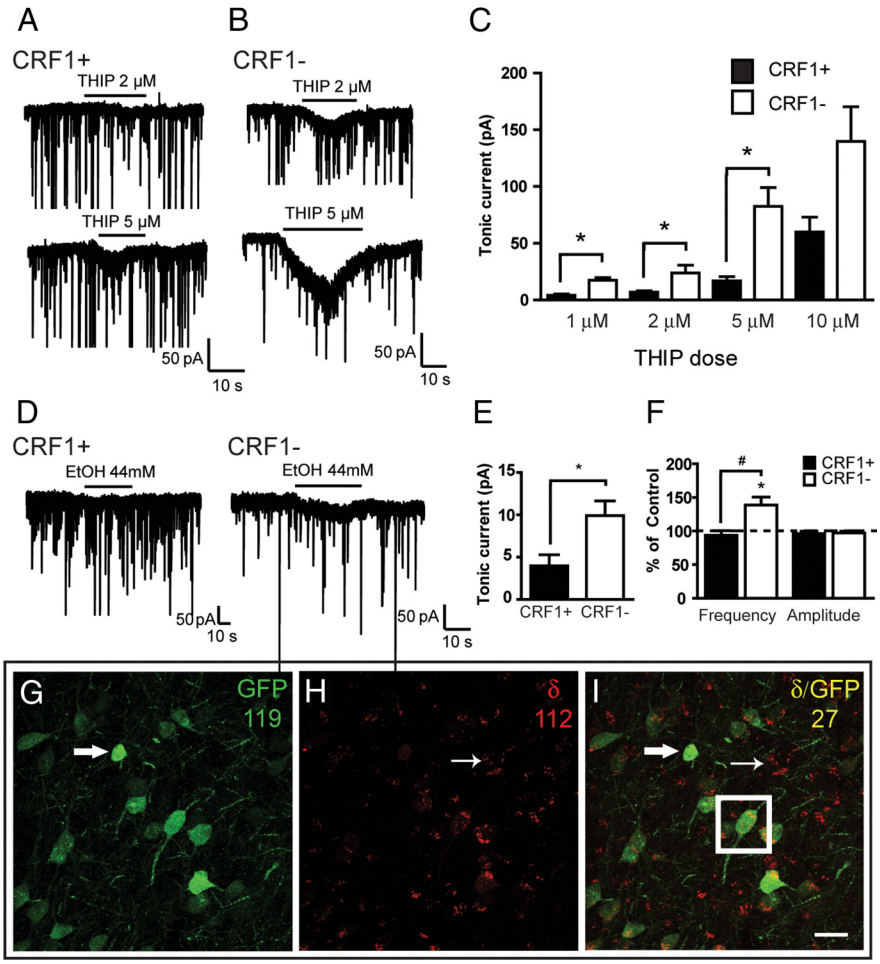

Figure 4. ***A***, Representative voltage-clamp recordings from a CRF1$^+$ neuron during focal application of 2 μM THIP (top trace) and 5 μM THIP (bottom trace). ***B***, Representative voltage-clamp recordings from a CRF1$^-$ neuron before and after focal application of 2 μM THIP (top trace) and 5 μM THIP (bottom trace). ***C***, Summary of the tonic current elicited by THIP (1–10 μM) in CRF1$^+$ and CRF1$^-$ neurons; $^*p < 0.05$ by unpaired *t* test, $n = 4, 6, 8$, and 3 (CRF1$^+$) and $n = 3, 5, 5$, and 3 (CRF1$^-$) for 1, 2, 5, and 10 μM THIP, respectively. ***D***, Representative voltage-clamp recordings from a CRF1$^+$ neuron (left trace) and a CRF1$^-$ neuron (right trace) during focal application of EtOH (44 mM). ***E***, Summary of the tonic current stimulated by EtOH (44 mM); $^*p < 0.05$ by unpaired *t* test, $n = 5$ (CRF1$^+$) and $n = 5$ (CRF1$^-$). ***F***, Summary of the change in sIPSC frequency and amplitude produced by EtOH (44 mM); $^*p < 0.05$ by one-sample *t* test, $n = 5$ (CRF1$^+$) and $n = 5$ (CRF1$^-$). ***G***, Photomicrograph (60×) of GFP expression (green fluorescence) and total number of CeA neurons that displayed GFP expression (119). Arrow indicates a GFP$^+$, CRF1-containing neuron. ***H***, Photomicrograph (60×) of δ $GABA_A$ receptor subunit expression (red punctate fluorescence) and total number of CeA neurons that displayed δ subunit expression (112). Arrow indicates a CRF1$^-$ neuron expressing the δ subunit. ***I***, Photomicrograph (60×) of merged GFP and δ subunit expression (green plus red fluorescence) and total number of CeA neurons that displayed both GFP and δ subunit expression (27). Arrows indicate the same CRF1$^+$ and CRF1$^-$ neurons as in ***G*** and ***H***. Box indicates a CRF1$^+$ neuron that expresses the δ subunit. Scale bar, 20 μm.

Cell-type-specific effects of EtOH on CeA neuron activity

Our voltage-clamp studies indicated that CRF1$^+$ neurons possess a tonic $GABA_A$ receptor conductance (Fig. 2) that is driven by action-potential-dependent GABA release (Fig. 3). However, the impact of changes in this cell-type-specific tonic conductance on the overall activity of CeA neurons cannot be determined in the voltage-clamp configuration. To determine the consequences of EtOH-induced changes in tonic conductance on the activity of both CRF1$^+$ and CRF1$^-$ neurons, we performed recordings using the extracellular cell-attached configuration. These recordings were performed using aCSF as the pipette solution so as not to artificially disturb the ionic balance of the neuronal membrane (Alcami et al., 2012). We only performed recordings on CeA neurons that displayed spontaneous firing with a regular discharge pattern so that changes in firing discharge could reliably be detected. CRF1$^+$ and CRF1$^-$ neurons that displayed no baseline firing discharge were observed, but no experiments were performed in these neurons.

To assess the effects of EtOH on firing discharge in CRF1$^+$ and CRF1$^-$ CeA neurons in a physiological environment, EtOH was superfused without any other pharmacological intervention (i.e., aCSF only). CRF1$^+$ neurons displayed an average baseline firing discharge frequency of 3.3 ± 1.7 Hz. Superfusion of EtOH (44 mM) onto CRF1$^+$ neurons significantly increased the firing discharge frequency to 224.5 ± 69.5% of baseline values ($p < 0.05$, $n = 6$; Fig. 6*A*,*C*). CRF1$^-$ neurons displayed an average baseline firing discharge frequency of 6.8 ± 2.3 Hz. Superfusion of EtOH (44 mM) onto CRF1$^-$ neurons significantly decreased the firing discharge frequency to 79.6 ± 6.8% of baseline values ($p < 0.05$, $n = 6$; Fig. 6*B*,*C*).

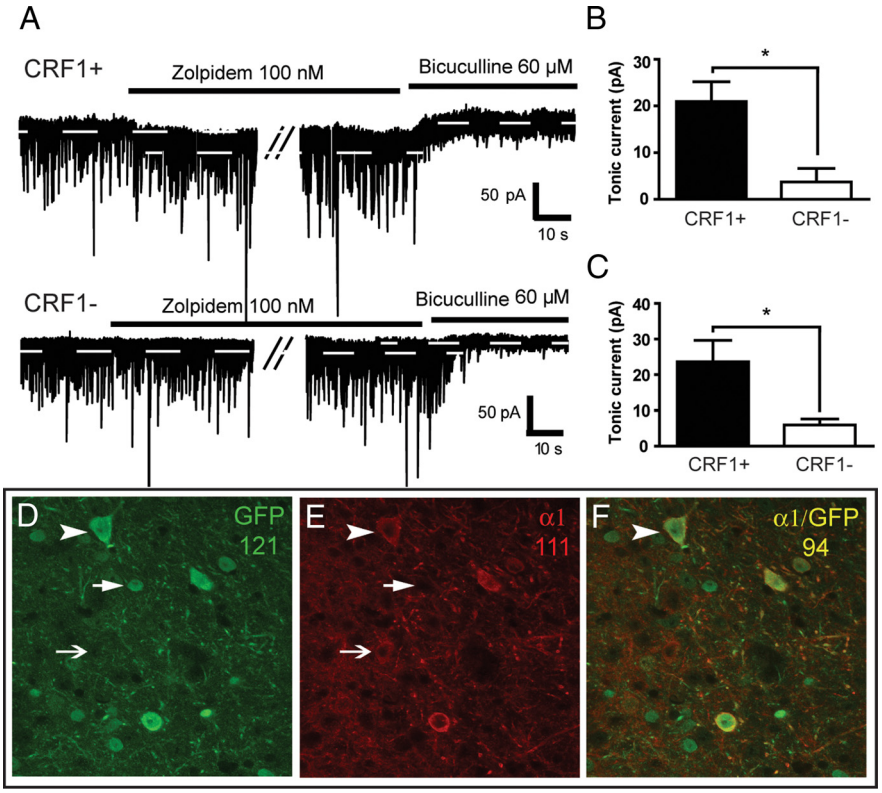

Figure 5. ***A***, Representative voltage-clamp recordings from a CRF1$^+$ neuron (top trace) and a CRF1$^-$ neuron (bottom trace) during superfusion of zolpidem (100 nM) followed by bicuculline (60 μM). Dashed lines indicate average holding current. ***B***, Summary of the tonic current produced by zolpidem superfusion in CRF1$^+$ neurons ($n = 6$) and CRF1$^-$ neurons ($n = 6$); *$p <$ 0.05 by unpaired *t* test. ***C***, Summary of the tonic current inhibited by subsequent bicuculline superfusion in CRF1$^+$ ($n = 6$) and CRF1$^-$ neurons ($n = 6$); *$p < 0.05$ by unpaired *t* test. ***D***, Photomicrograph (60×) of GFP expression (green fluorescence) and total number of CeA neurons quantified as displaying GFP expression (121). Arrows indicate CRF1$^+$ neurons (top and middle arrows) and a CRF1$^-$ neuron (bottom arrow). ***E***, Photomicrograph (60×) of α1 GABA$_A$ receptor subunit expression (red fluorescence) and total number of CeA neurons that displayed α1 subunit expression (111). Arrows are the same as in ***D*** showing α1 subunit expression (top and bottom arrow) and lack of α1 subunit expression (middle arrow). ***F***, Photomicrograph (60×) of merged GFP and α1 subunit expression (green and red fluorescence) and total number of CeA neurons that displayed both GFP and α1 subunit expression (94). Arrows are the same as in ***D*** and ***E***. Scale bar, 20 μm.

Based on the importance of GABA transmission in the CeA and the distinct effects of EtOH on CRF1$^+$ and CRF1$^-$ CeA neurons, we hypothesized that changes in GABA$_A$ receptor activity mediated the differential effects of EtOH on CRF1$^+$ and CRF1$^-$ neurons. To assess this hypothesis, we performed cell-attached recordings in the presence of the glutamate receptor antagonists DNQX and AP-5 and the GABA$_B$ receptor antagonist CGP to pharmacologically isolate GABA$_A$ receptor activity. In the presence of DNQX, AP-5, and CGP, CRF1$^+$ neurons displayed an average baseline firing rate of 9.6 ± 3.7 Hz. Superfusion of EtOH (44 mM) onto CRF1$^+$ neurons in the presence of DNQX, AP-5, and CGP significantly increased the rate of firing discharge to 213.2 ± 38.1% of control values ($p < 0.05$, $n = 5$; Fig. 6*D*,*F*). In the presence of DNQX, AP-5, and CGP, CRF1$^-$ neurons displayed an average baseline firing rate of 3.7 ± 1.0 Hz. Superfusion of EtOH (44 mM) in the presence of DNQX, AP-5, and CGP significantly decreased the firing discharge rate to 34.4 ± 7.6% of control values in five of six CRF1$^-$ neurons ($p < 0.05$; Fig. 6*E*,*F*). One CRF1$^-$ neuron displayed an average baseline firing rate of 6.0 ± 1.1 Hz, and superfusion of EtOH increased the firing rate to 125.2% of control. This neuron was excluded from the group analysis because it likely reflects a distinct subpopulation of CRF1$^-$ neurons. Collectively, these data suggest that the EtOH effects on firing rate in CRF1$^+$ and CRF1$^-$ neurons are mediated by GABA$_A$ receptors, although the variability in CRF1$^-$ neurons likely reflects the heterogeneity of the CRF1$^-$ population.

To further examine the hypothesis that GABA$_A$ receptors mediate the effects of EtOH on firing rate of CRF1$^+$ and CRF1$^-$ CeA neurons, we performed cell-attached recordings in the presence of DNQX, AP-5, and CGP and superfused the GABA$_A$ receptor antagonist GBZ, followed by EtOH in the presence of GBZ. CRF1$^+$ neurons displayed an average firing rate of 5.5 ± 3.9 Hz. Superfusion of GBZ (100 μM) onto CRF1$^+$ neurons significantly increased the firing discharge rate to 256.7 ± 56.2% of control values ($p < 0.05$, $n = 5$, Fig. 7*A*,*C*). Subsequent superfusion of EtOH (44 mM) in the presence of GBZ produced no significant change in firing rate (102.8 ± 6.5% of control values, $n = 5$; Fig. 7*A*,*D*). CRF1$^-$ neurons displayed an average baseline firing rate of 5.2 ± 2.1 Hz. Superfusion of GBZ (100 μM) did not significantly change the firing discharge rate in four of six CRF1$^-$ neurons (80.0 ± 20% of control; Fig. 7*B*,*C*) but did significantly increase the firing rate in two of six CRF1$^-$ neurons that were not included in the analysis. Subsequent superfusion of EtOH (44 mM) in the presence of GBZ produced no significant change in firing rate in five of five CRF1$^-$ neurons (114.2 ± 5.8% of control values; Fig. 7*B*,*D*). Together, these data further suggest that the differential effects of EtOH on CRF1$^+$ and CRF1$^-$ CeA neurons are mediated by GABA$_A$ receptors.

Local synaptic connectivity of CRF1$^+$ and CRF1$^-$ CeA neurons

One possible mechanism for the cell-type-specific effects of EtOH on firing discharge is that a cell-type-specific alteration of local GABAergic signaling by EtOH occurs such that EtOH stimulates tonic inhibition of CRF1$^-$ neurons that synapse onto CRF1$^+$ neurons, resulting in a disinhibition of CRF1$^+$ neurons and increased firing. To test the hypothesis that CRF1$^-$ neurons form local synapses onto CRF1$^+$ neurons, we performed simultaneous recordings in CRF1$^-$ and CRF1$^+$ neurons in close proximity (Fig. 8*A*,*B*). To examine local synaptic connectivity, one neuron was placed in current-clamp configuration and subjected to brief (10 ms) current injections (400–600 pA) to elicit one to two action potential spikes. The other neuron was placed in voltage-clamp mode and held at −60 mV. A total of 25 simultaneous dual recordings were performed, and, of those, only 1 of 25 displayed synaptic coupling of an IPSC in a CRF1$^+$ neuron to a stimulated action potential in a CRF1$_-$ neuron (Fig. 8*C*). A synaptically coupled IPSC was observed in 5 of 10 sweeps of current injection (Fig. 8*C*, gray traces) that were averaged (Fig. 8*E*, black trace) and displayed an average latency of 1 ms and an average amplitude of 13.8 pA. Spontaneous action potentials were observed in all CRF1$_-$ neurons recorded and significantly compli-

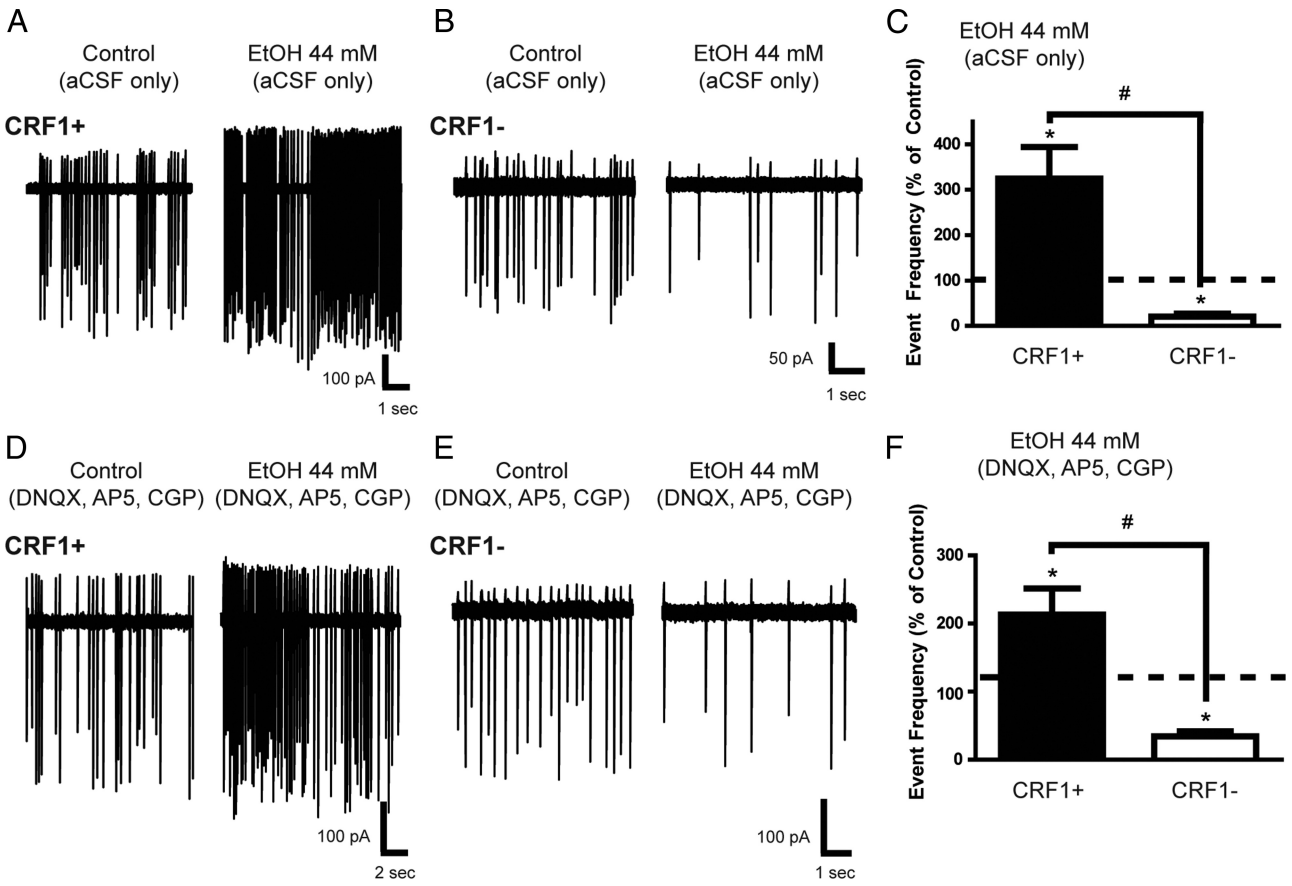

Figure 6. ***A***, Representative cell-attached recording from a CRF1$^+$ neuron before (left trace) and during (right trace) superfusion of EtOH in physiological conditions (EtOH 44 mM, aCSF only). ***B***, Representative cell-attached recording from a CRF1$^-$ neuron before (left trace) and during (right trace) superfusion of EtOH in physiological conditions (EtOH 44 mM, aCSF only). ***C***, Summary of the change in event frequency (% of Control) in CRF1$^+$ neurons ($n = 6$) and CRF$^-$ neurons ($n = 6$) before and during EtOH superfusion in physiological condition (aCSF only); $^*p < 0.05$ by one-sample *t* test, $^\#p < 0.05$ by unpaired *t* test. ***D***, Representative cell-attached recording from a CRF1$^+$ neuron before (left trace) and during (right trace) superfusion of EtOH with pharmacological isolation of $GABA_A$ receptor transmission (DNQX, AP-5, CGP). ***E***, Representative cell-attached recording from a CRF1$^-$ neuron before (left trace) and during (right trace) superfusion of EtOH with pharmacological isolation of $GABA_A$ receptor transmission (DNQX, AP-5, CGP). ***F***, Summary of the change in event frequency (% of Control) in CRF1$^+$ neurons ($n = 5$) and CRF$^-$ neurons ($n = 5$) before and during EtOH superfusion with pharmacological isolation of $GABA_A$ receptor transmission (DNQX, AP-5, CGP); $^*p < 0.05$ by one-sample *t* test, $^\#p < 0.05$ by unpaired *t* test.

cated the measurement of action potential/IPSC coupling. In 8 of 25 recordings, the configuration was reversed such that the CRF1$^+$ neuron was recorded in current clamp and stimulated by a brief current injection, and the CRF1$^-$ neurons was recorded in voltage clamp. No synaptically coupled action potentials and IPSCs were observed in this configuration.

The apparent connectivity of CRF1$^-$ and CRF1$^+$ neurons in these initial studies was low (4%) and weak (<20 pA). To determine whether the incidence and strength of synaptic coupling was negatively impacted by Ca^{2+} buffering in the intracellular solution, we performed dual recordings with decreased Ca^{2+} buffering (1 mM EGTA in the intracellular solution). A total of eight dual recordings were performed as described above, and four of eight displayed synaptic coupling of an IPSC in a CRF1$^+$ neuron to a stimulated action potential in a CRF1$^-$ neuron. Synaptically coupled IPSCs were observed in ~50% of sweeps and displayed an average latency of 2.3 ± 0.8 ms and an average amplitude of 36.1 ± 5.8 pA (Fig. 8*D*). Spontaneous action potentials were observed in all CRF1$^-$ neurons recorded, but the frequency of action potentials was not significantly different from that observed in the original Ca^{2+} buffered conditions. In eight of eight recordings, the configuration was reversed, and no synaptically coupled action potentials and IPSCs were observed. Although the variability and instability of this local synaptic transmission precluded the examination of the effects of EtOH, these data demonstrate that CRF1$^-$ neurons form inhibitory synapses onto CRF1$^+$ neurons in the CeA and suggest that there are no reciprocal connections.

CRF1 neurons in local CeA microcircuitry and extended amygdala

Based on the morphology of CRF1$^+$ neurons and the differential effects of EtOH on the firing discharge of CRF1$^+$ and CRF1$^-$ neurons, we hypothesized that CRF1$^+$ neurons project out of the CeA to other targets in the extended amygdala. A main projection target of the CeA (particularly the medial portion) is the BNST (Dong et al., 2001), and the CeA is a major source of CRF in the BNST (Sakanaka et al., 1986). To determine whether CRF1$^+$ neurons from the CeA project to the BNST, we used fluorescent microspheres to retrogradely label neurons in the CeA and performed immunohistochemistry to determine whether there was colocalization with GFP in CRF1$^+$ neurons. Injection of red fluorescent microspheres into the dlBNST (Fig. 9*A*) of four mice resulted in retrograde transport of microspheres to the CeA, particularly the medial portion (Fig. 9*B*). We detected colocalization of red fluorescent microspheres and GFP in 30.5 ± 2.9% of all CRF1$^+$ neurons in the CeA (Fig. 9*C*), indicating that these neurons do project out of the CeA and that the dlBNST is at least one

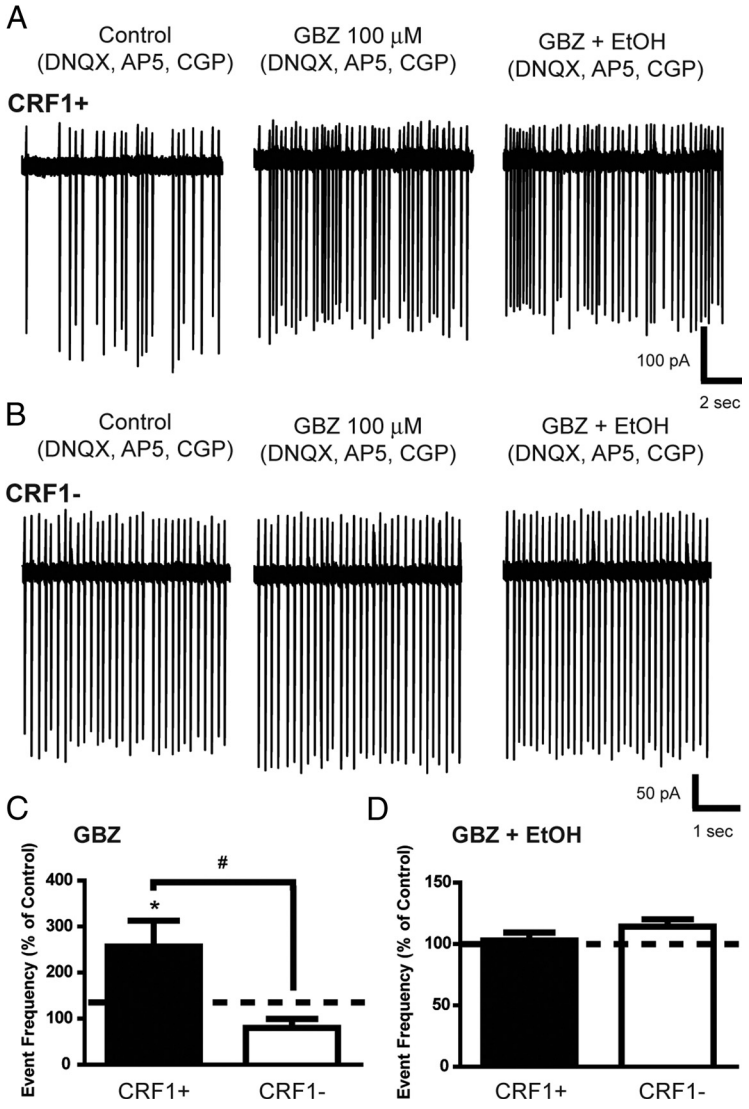

Figure 7. ***A***, Representative cell-attached recording from a CRF1$^+$ neuron in control conditions (left trace), during superfusion of GBZ (100 μM; middle trace), and during superfusion of EtOH in the presence of gabazine (GBZ + EtOH, right trace). All recordings were performed with pharmacological isolation of $GABA_A$ receptor transmission (DNQX, AP-5, CGP). ***B***, Representative cell-attached recording from a CRF1$^-$ neuron in control conditions (left trace), during superfusion of GBZ (100 μM; middle trace), and during superfusion of EtOH in the presence of gabazine (GBZ + EtOH, right trace). All recordings were performed with pharmacological isolation of $GABA_A$ receptor transmission (DNQX, AP-5, CGP). ***C***, Summary of the change in event frequency (% of Control) in CRF1$^+$ neurons ($n = 5$) and CRF1$^-$ neurons ($n = 5$) before and during GBZ (100 μM) superfusion. $^*p < 0.05$ by one-sample *t* test, $^{\#}p < 0.05$ by unpaired *t* test. ***D***, Summary of the change in event frequency (% of Control) in CRF1$^+$ neurons ($n = 5$) and CRF1$^-$ neurons ($n = 5$) before and during superfusion of EtOH in the presence of GBZ (GBZ + EtOH). $^*p < 0.05$ by one-sample *t* test, $^{\#}p < 0.05$ by unpaired *t* test.

of their downstream targets. The percentage of CRF1$^+$ neurons containing microspheres may be an underestimation because of the impossibility of injecting microspheres throughout the entire dlBNST. Microspheres were also detected in CRF1$^-$ neurons in the CeA, but quantification of these neurons was prevented by the variability of microsphere content and an inability to clearly delineate CRF1$^-$ cell bodies. CRF1$^-$ neurons containing microspheres likely reflect a separate subpopulation of CeA neurons that also project to the dlBNST.

To test the hypothesis that EtOH selectively excites CRF1$^+$ neurons that project out of the CeA, we infused microspheres into the dlBNST of six mice (Fig. 9*D*,*E*) and performed cell-attached recordings in CRF1$^+$ and CRF1$^-$ neurons from these mice that contained microspheres retrogradely transported from the dlBNST (Fig. 9*D*,*E*). CRF1$^+$ neurons that also expressed microspheres displayed an average baseline firing rate of 2.2 ± 0.7 Hz. Superfusion of EtOH (44 mM) significantly increased the firing discharge rate to 3.7 ± 1.1 Hz (242.5 ± 86.6% of control, $p < 0.05$, $n = 6$; Fig. 9*F*,*G*). CRF1$^-$ neurons that also expressed microspheres displayed an average baseline firing rate of 3.2 ± 1.5 Hz. Superfusion of EtOH (44 mM) significantly increased the firing discharge rate to 5.5 ± 2.0 Hz (252.4 ± 61.8% of control, $p < 0.05$, $n = 4$; Fig. 9*H*,*I*). These data suggest that EtOH increases the firing rate of all CeA neurons that project out of the CeA into the dlBNST and that CRF1$^+$ neurons make up at least one of these populations.

Discussion

The results of these studies indicate that the CeA has two subunit-specific forms of tonic inhibition that are anatomically and functionally distinct, with differential responses to acute EtOH. CRF1$^+$ neurons exhibited an ongoing tonic conductance mediated by the α1 $GABA_A$ receptor subunit that is driven by action-potential-dependent GABA release and likely occurs at receptors located in or near the synapse. In contrast, CRF1$^-$ neurons display no ongoing tonic inhibition but demonstrate a δ subunit-mediated tonic conductance in the presence of increased local GABA concentration that is selectively enhanced by acute EtOH and likely occurs at extrasynaptic receptors. EtOH increased the firing discharge of CRF1$^+$ neurons and decreased the firing discharge of CRF1$^-$ neurons through differential actions on local $GABA_A$ receptor signaling. Paired recordings indicate that CRF1$^-$ neurons form local synapses onto CRF1$^+$ neurons in the CeA. Retrograde tracing indicated that CeA CRF1$^+$ neurons project into the BNST and that these neurons are excited by EtOH. Importantly, EtOH increased the firing discharge of all neurons (CRF1$^+$ and CRF1$^-$) that project out of the CeA into the dlBNST, suggesting that the excitatory effects of EtOH may be more relevant to circuitry than to a specific subpopulation. Integration of the functional and anatomical data suggests that there is a local inhibitory microcircuit in the CeA wherein intrinsic CRF1$^-$ neurons provide local inhibition to CRF1$^+$ neurons that project out of the CeA into the BNST. Furthermore, the data suggest that EtOH augments the tonic inhibition on local CRF1$^-$ neurons, resulting in disinhibition and increased firing discharge of CRF1$^+$ output neurons. A schematic of this proposed CeA microcircuitry is shown in Figure 10.

$GABA_A$ receptor signaling has two distinct forms that function in a cell- and region-specific manner. Phasic signaling involves the generation of individual IPSCs that are the result of

"point-to-point" transmission that occurs at synapses and results in 10–100 ms of inhibition. Tonic signaling is characterized by the presence of persistent inhibitory currents that are the result of GABA acting at highly sensitized $GABA_A$ receptors (for review, see Glykys and Mody, 2007a; Belelli et al., 2009). A recent study described cell-type-specific tonic inhibition in the lateral and basolateral amygdala that was mediated by $GABA_A$ receptors containing the $\alpha 3$ subunit (Marowsky et al., 2012). This study is the first to demonstrate the presence of tonic conductance in CeA neurons and to demonstrate cell-type-specific tonic signaling within the CeA. The tonic signaling in $CRF1^+$ and $CRF1^-$ neurons is mediated by $GABA_A$ receptors with different subunit compositions and distinct functional properties. $CRF1^+$ neurons possess an ongoing tonic conductance that is dramatically reduced by blockade of action-potential-dependent GABA release with TTX. The decrease in IPSC frequency with TTX is positively correlated with the magnitude of the decrease in tonic conductance. In addition, the tonic conductance in $CRF1^+$ neurons is augmented by a low concentration of zolpidem, suggesting the presence of a $\alpha 1$ subunit in these $GABA_A$ receptors. Previous studies have shown that the $\alpha 1$ $GABA_A$ receptor subunit is expressed in the CeA (Pirker et al., 2000), and here we show that the $\alpha 1$ subunit is expressed predominantly (although not exclusively) in $CRF1^+$ CeA neurons.

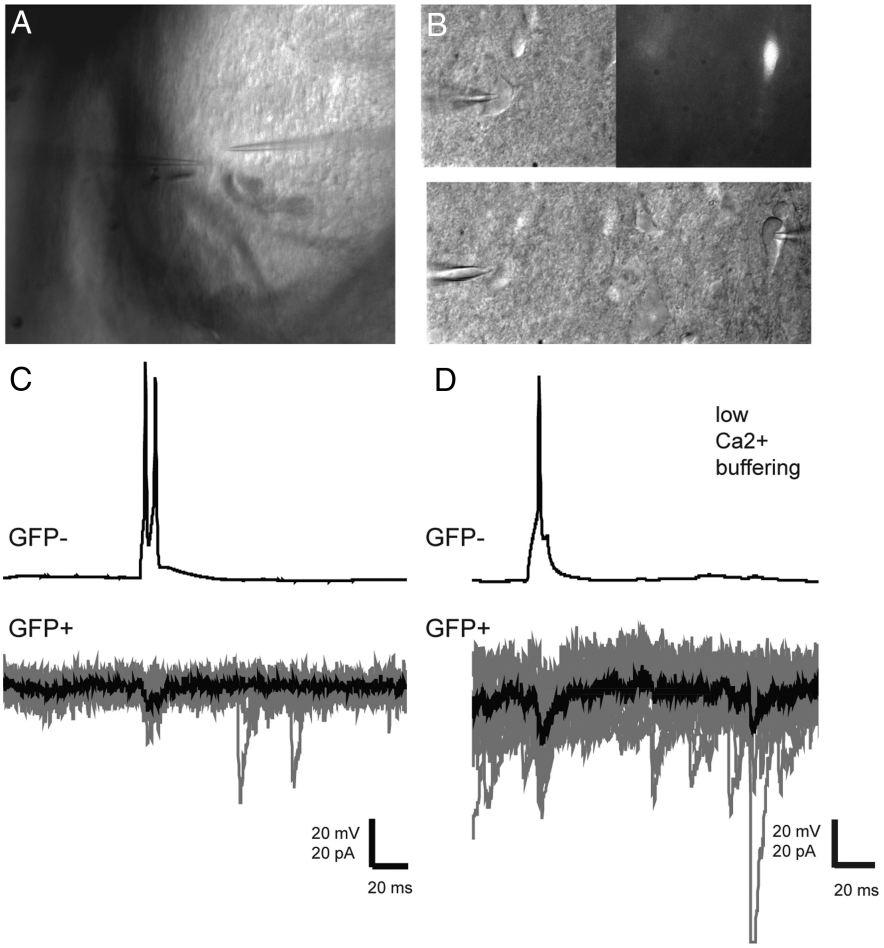

Figure 8. ***A***, Photomicrograph (10×) of a CeA slice during a paired recording. ***B***, Photomicrographs (60×) of synaptically coupled $CRF1^-$ (left) and $CRF1^+$ (right) CeA neurons. ***C***, Representative traces of an action potential elicited from a $CRF1^-$ neuron (top trace) and superimposed (gray traces) and averaged (black trace) IPSCs from a synaptically coupled $CRF1^+$ neuron (bottom trace). ***D***, Representative traces of an action potential elicited from a $CRF1^-$ neuron (top trace) and superimposed (gray traces) and averaged (black trace) IPSCs from a synaptically coupled $CRF1^+$ neuron (bottom trace) recorded using a low Ca^{2+} buffered intracellular solution.

In contrast to the findings in $CRF1^+$ neurons, the tonic $GABA_A$ receptors located on $CRF1^-$ neurons are not active in the basal state but can be stimulated by blockade of GABA reuptake. This positions the tonic signaling in $CRF1^-$ neurons to be sensitive to physiological conditions in which local GABA concentrations are elevated, for example, after chronic EtOH exposure (Roberto et al., 2003). In addition, this tonic conductance is acutely stimulated by pharmacological agents, such as THIP or EtOH, suggesting the presence of the δ subunit (Wei et al., 2004; Drasbek and Jensen, 2006; Glykys et al., 2007). Previous studies found δ subunit expression in the CeA, although at very low levels (Pirker et al., 2000). Our immunohistochemical studies confirm the presence of the δ subunit and show that it is found primarily in $CRF1^-$ CeA neurons. The δ $GABA_A$ receptor subunit in $CRF1^-$ neurons likely pairs with a $\alpha 4$ or $\alpha 6$ subunit. It is possible that the EtOH-sensitive tonic conductance observed in $CRF1^-$ neurons is mediated by $GABA_A$ receptors that contain both the $\alpha 1$ and δ subunits, as has been shown in the hippocampus (Glykys et al., 2007). However, we do not believe that this subunit assembly is present in the CeA or is only present in small amounts, because the $\alpha 1$ subunit was primarily detected in $CRF1^+$ neurons and $CRF1^-$ neurons were not sensitive to the effects of zolpidem, suggesting that the $\alpha 1$ subunit is not present in these neurons. The distinct anatomical and functional properties of the different types of tonic conductance found in $CRF1^+$ and $CRF1^-$ neurons in the CeA is consistent with previous work demonstrating that inhibition generated by synaptic spillover is mediated by a distinct receptor population than that generated by ambient GABA and that the δ subunit is associated solely with ambient GABA in the extrasynaptic space, not synaptic spillover (Bright et al., 2011).

It has been shown previously that EtOH induces neuroadaptive changes in GABA signaling in the CeA (Roberts et al., 1996; Roberto et al., 2003, 2004) and that these effects can be blocked by CRF1 antagonists (Roberto et al., 2010). However, the CeA circuitry underlying these effects remains unclear. We showed previously that EtOH increases action-potential-independent GABA release in the majority of CeA neurons by acting at presynaptic CRF1 receptors (Nie et al., 2004; Bajo et al., 2008). Here, we examined spontaneous GABA release and the firing output of CeA neurons to better interpret EtOH-induced changes in synaptic transmission in the context of overall CeA network activity. Consistent with our previous findings on action-potential-independent GABA release, we observed that acute EtOH increased spontaneous GABA release onto $CRF1^-$ neurons. However, in the present study, we found that acute EtOH produced no change in spontaneous GABA release onto $CRF1^+$ neurons. Because it was not possible to identify $CRF1^+$ neurons in our previous studies and because these neurons make up only a small portion of the overall CeA neuronal population, it is likely

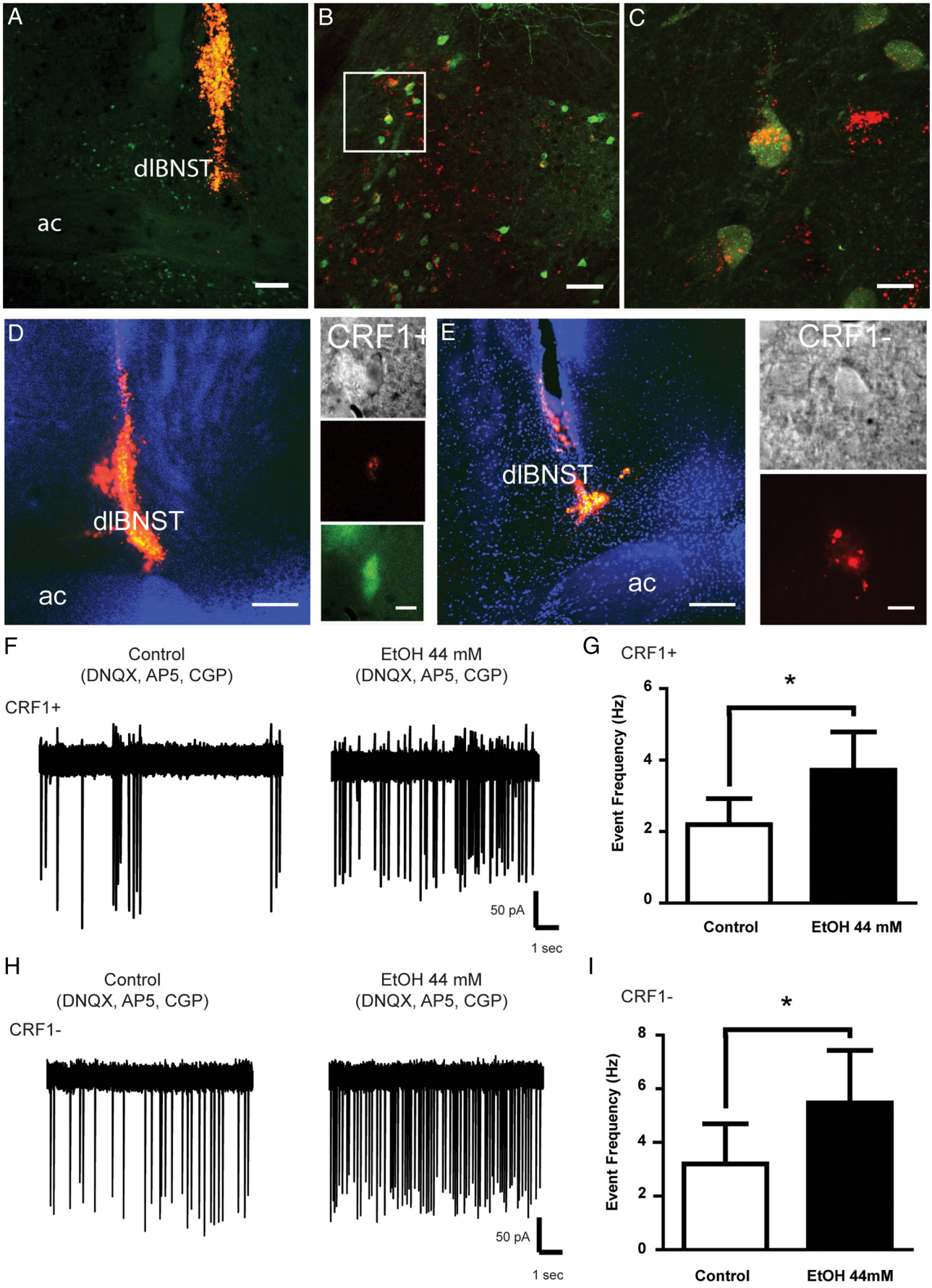

Figure 9. ***A***, Photomicrograph (20×) of microsphere injection site into the dlBNST dorsal and lateral to the anterior commissure (ac). Scale bar, 100 μm. ***B***, Photomicrograph (25×) of retrogradely transported red microspheres (red punctate fluorescence) and CRF1 $^{+}$ neurons (green fluorescence) in the CeA of the same brain shown in ***A***. Scale bar, (*Figure legend continues.*)

that these neurons were not well represented in the previous experimental samples. We speculate that the neuronal population represented in our previous studies was primarily composed of CeA interneurons and that CeA projection neurons made up the small proportion of our previous sample that did not show a change in GABA release in response to acute EtOH.

The studies examining firing discharge provide additional information as to the effects of acute EtOH on specific components of the CeA microcircuitry. Superfusion of acute EtOH elicited opposing effects on firing discharge in CRF1$^+$ and CRF1$^-$ neurons, both of which were mediated by the $GABA_A$ receptor. The decrease in firing discharge observed in CRF1$^-$ neurons could be the result of EtOH-induced enhanced phasic and tonic $GABA_A$ receptor inhibition that was observed in these neurons. The increase in firing discharge in CRF1$^+$ neurons is less clear. It is possible that the increase in firing discharge is the result of indirect effects of EtOH on other neurotransmitter systems. However, based on the cell-type-specific effects of EtOH on GABA signaling and the importance of GABA transmission in overall CeA activity, we propose that the differential effects of acute EtOH are the result of local inhibitory connections within the CeA wherein a population of local CRF1$^-$ interneurons regulates the activity of CRF1$^+$ neurons that project out of the CeA (Fig. 10). Acute EtOH stimulates tonic signaling in CRF1$^-$ neurons (likely through direct effects of EtOH on δ-containing $GABA_A$ receptors) and increases GABA release onto these neurons, resulting in decreased firing discharge. The enhanced tonic inhibition of these CRF1$^-$ neurons results in disinhibition of the CRF1$^+$ CeA neurons, which produces a more excitable state and increased firing discharge. Because the CRF1$^+$ neurons project out of the CeA into the BNST, we presume that acute EtOH results in increased GABA release at the level of the BNST.

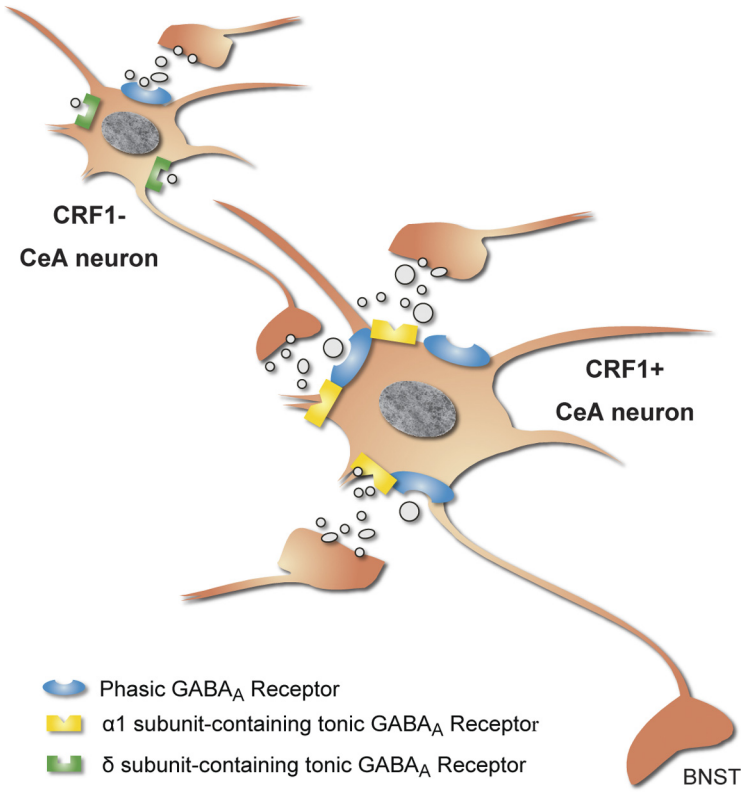

Figure 10. Proposed microcircuitry of the CeA illustrating local phasic and tonic $GABA_A$ receptor transmission in CRF1$^+$ and CRF1$^-$ neurons. Phasic $GABA_A$ receptor transmission is depicted on both CRF1$^+$ and CRF1$^-$ neurons, although CRF1$^+$ neurons are depicted with more baseline GABA activity. The CRF1$^+$ neuron possesses α1 subunit-containing tonic $GABA_A$ receptors located in or near the synaptic cleft to reflect the dependence on action-potential-dependent GABA release and projects out of the CeA into the BNST. The CRF1$^-$ neuron possesses δ subunit-containing $GABA_A$ receptors located outside the synaptic cleft to reflect activation by ambient GABA. We hypothesize that EtOH acts on this CeA circuitry by enhancing tonic conductance in CRF1$^-$ neurons through actions at δ-containing $GABA_A$ receptors, resulting in decreased firing of this subpopulation. The ongoing tonic inhibition of CRF1$^+$ neurons is subsequently diminished, resulting in disinhibition and increased firing in this subpopulation. This increased firing then results in increased GABA release in target brain regions, such as the BNST.

Tonic $GABA_A$ receptor currents have been shown to have an increased sensitivity to EtOH, prompting some researchers to suggest that tonic receptors are the primary target for EtOH in the brain (Wallner et al., 2003; Mody et al., 2007; Belelli et al., 2009). At low concentrations, EtOH has been shown to potentiate the function of $GABA_A$ receptors containing the δ subunit associated with the α4 or α6 subunit (Wallner et al., 2003), although this direct action of EtOH on tonic $GABA_A$ receptors remains controversial (Borghese and Harris, 2007; Botta et al., 2007; Baur et al., 2009). The proposed EtOH antagonist Ro 15-4513 (ethyl-8-azido-5,6-dihydro-5-methyl-6-oxo-4*H*-imidazo[1,5α][1,4]benzodiazepine-3-carboxylate) has been shown by some to act at the γ2 benzodiazepine $GABA_A$ receptor site (Luddens and Wisden, 1991; Linden et al., 2011) and by others to act at α4/6βδ $GABA_A$ receptors (Hanchar et al., 2006; Wallner et al., 2006). The α1 subunit of the $GABA_A$ receptor has also been implicated as a target of alcohol-associated neuroadaptation. Notably, α1 subunit levels are significantly higher in the CeA of high alcohol drinking rats compared with low alcohol drinking controls (Yang et al., 2011). In addition, mice with a genetic deletion of the α1 subunit display significantly decreased alcohol drinking (June et al., 2007). These results suggest that neuroplastic changes in δ and α1 subunit expression and/or function occur with alcohol exposure. In addition, the augmentation of

←

(*Figure legend continued.*) 50 μm. ***C***, Photomicrograph (180×) of the CRF1$^+$ CeA neuron with red microsphere labeling indicated by the white box in ***B***. Scale bar, 10 μm. ***D***, Photomicrograph of the microsphere injection site into the dlBNST (left). Scale bar, 100 μm. Photomicrographs (60×) of a CRF1$^+$ CeA neuron from the same brain in IR-DIC (top right), red fluorescence (middle right), and green fluorescence (bottom right). Scale bar, 10 μm. ***E***, Photomicrograph of the microsphere injection site into the dlBNST (left). Scale bar, 100 μm. Photomicrographs (60×) of a CRF1$^-$ CeA neuron from the same brain in IR-DIC (top right) and red fluorescence (bottom right). Scale bar, 10 μm. ***F***, Representative cell-attached recording from a CRF1$^+$ neuron containing microspheres before (left trace) and during (right trace) superfusion of EtOH with pharmacological isolation of $GABA_A$ receptor transmission (EtOH 44 mM; DNQX, AP-5, CGP). ***G***, Summary of the event frequency in CRF1$^+$ neurons containing microspheres during control and during EtOH superfusion. *$p < 0.05$ by unpaired *t* test. ***H***, Representative cell-attached recording from a CRF1$^-$ neuron containing microspheres before (left trace) and during (right trace) superfusion of EtOH with pharmacological isolation of $GABA_A$ receptor transmission (EtOH 44 mM; DNQX, AP-5, CGP). ***I***, Summary of the event frequency in CRF1$^-$ neurons containing microspheres during control and during EtOH superfusion. *$p < 0.05$ by unpaired *t* test.

the tonic conductance in CRF1$^+$ neurons by zolpidem presents the possibility that additional dysregulation of CeA circuitry could result from the combined use of EtOH and benzodiazepines. This compound dysregulation of CeA circuitry could be implicated in the additional complications of polydrug abuse.

The divergent effects that different pharmacological agents (including EtOH) have on CRF1$^+$ compared with CRF1$^-$ neurons highlight the importance of identifying specific cell types and populations in interpreting cellular data from the CeA. These data demonstrate the need for additional characterization of distinct CeA neuronal populations and local microcircuits to examine how perturbations in cell signaling within the CeA affect the activity of the extended amygdala to produce disorders such as alcohol dependence. Because tonic signaling is a critical determinant of overall network activity and tone (Semyanov et al., 2004), the differential tonic conductance in discrete populations of CeA neurons allows for multiple levels of network regulation. The organization and fine-tuned control of these inhibitory microcircuits in the CeA likely account for the ability of the CeA to integrate such disparate inputs (stress, anxiety, fear, reinforcement) with the appropriate behavioral outputs. However, the multiple populations and levels of control within these local microcircuits also provide many targets for dysregulation and the pathological conditions that result (e.g., alcohol dependence).

References

Ade KK, Janssen MJ, Ortinski PI, Vicini S (2008) Differential tonic GABA conductances in striatal medium spiny neurons. J Neurosci 28:1185–1197. CrossRef Medline

Alcami P, Franconville R, Llano I, Marty A (2012) Measuring the firing rate of high-resistance neurons with cell-attached recording. J Neurosci 32: 3118–3130. CrossRef Medline

Alheid GF, Heimer L (1988) New perspectives in basal forebrain organization of special relevance for neuropsychiatric disorders: the striatopallidal, amygdaloid, and corticopetal components of substantia innominata. Neuroscience 27:1–39. CrossRef Medline

Bajo M, Cruz MT, Siggins GR, Messing R, Roberto M (2008) Protein kinase C epsilon mediation of CRF- and ethanol-induced GABA release in central amygdala. Proc Natl Acad Sci U S A 105:8410–8415. CrossRef Medline

Baur R, Kaur KH, Sigel E (2009) Structure of alpha6 beta3 delta GABA(A) receptors and their lack of ethanol sensitivity. J Neurochem 111:1172–1181. CrossRef Medline

Belelli D, Harrison NL, Maguire J, Macdonald RL, Walker MC, Cope DW (2009) Extrasynaptic GABAA receptors: form, pharmacology, and function. J Neurosci 29:12757–12763. CrossRef Medline

Borghese CM, Harris RA (2007) Studies of ethanol actions on recombinant delta-containing gamma-aminobutyric acid type A receptors yield contradictory results. Alcohol 41:155–162. CrossRef Medline

Botta P, Radcliffe RA, Carta M, Mameli M, Daly E, Floyd KL, Deitrich RA, Valenzuela CF (2007) Modulation of GABAA receptors in cerebellar granule neurons by ethanol: a review of genetic and electrophysiological studies. Alcohol 41:187–199. CrossRef Medline

Bright DP, Renzi M, Bartram J, McGee TP, MacKenzie G, Hosie AM, Farrant M, Brickley SG (2011) Profound desensitization by ambient GABA limits activation of delta-containing GABAA receptors during spillover. J Neurosci 31:753–763. CrossRef Medline

Caraiscos VB, Elliott EM, You-Ten KE, Cheng VY, Belelli D, Newell JG, Jackson MF, Lambert JJ, Rosahl TW, Wafford KA, MacDonald JF, Orser BA (2004) Tonic inhibition in mouse hippocampal CA1 pyramidal neurons is mediated by alpha5 subunit-containing gamma-aminobutyric acid type A receptors. Proc Natl Acad Sci U S A 101:3662–3667. CrossRef Medline

Carta M, Mameli M, Valenzuela CF (2004) Alcohol enhances GABAergic transmission to cerebellar granule cells via an increase in Golgi cell excitability. J Neurosci 24:3746–3751. CrossRef Medline

Chieng BC, Christie MJ, Osborne PB (2006) Characterization of neurons in the rat central nucleus of the amygdala: cellular physiology, morphology, and opioid sensitivity. J Comp Neurol 497:910–927. CrossRef Medline

Chu K, Koob GF, Cole M, Zorrilla EP, Roberts AJ (2007) Dependence-induced increases in ethanol self-administration in mice are blocked by the CRF1 receptor antagonist antalarmin and by CRF1 receptor knockout. Pharmacol Biochem Behav 86:813–821. CrossRef Medline

Debanne D, Boudkkazi S, Campanac E, Cudmore RH, Giraud P, Fronzaroli-Molinieres L, Carlier E, Caillard O (2008) Paired-recordings from synaptically coupled cortical and hippocampal neurons in acute and cultured brain slices. Nat Protoc 3:1559–1568. CrossRef Medline

Dong HW, Petrovich GD, Swanson LW (2001) Topography of projections from amygdala to bed nuclei of the stria terminalis. Brain Res Brain Res Rev 38:192–246. CrossRef Medline

Drasbek KR, Jensen K (2006) THIP, a hypnotic and antinociceptive drug, enhances an extrasynaptic GABAA receptor-mediated conductance in mouse neocortex. Cereb Cortex 16:1134–1141. CrossRef Medline

Dumont EC, Martina M, Samson RD, Drolet G, Par é D (2002) Physiological properties of central amygdala neurons: species differences. Eur J Neurosci 15:545–552. CrossRef Medline

Franklin KBJ, Paxinos G (2008) The mouse brain atlas in stereotaxic coordinates, Ed 3. New York: Elsevier.

Funk CK, Zorrilla EP, Lee MJ, Rice KC, Koob GF (2007) Corticotropin-releasing factor 1 antagonists selectively reduce ethanol self-administration in ethanol-dependent rats. Biol Psychiatry 61:78–86. CrossRef Medline

Glykys J, Peng Z, Chandra D, Homanics GE, Houser CR, Mody I (2007) A new naturally occurring GABA(A) receptor subunit partnership with high sensitivity to ethanol. Nat Neurosci 10:40–48. CrossRef Medline

Glykys J, Mody I (2007a) Activation of GABAA receptors: views from outside the synaptic cleft. Neuron 56:763–770. CrossRef Medline

Glykys J, Mody I (2007b) The main source of ambient GABA responsible for tonic inhibition in the mouse hippocampus. J Physiol 582:1163–1178. CrossRef Medline

Glykys J, Mann EO, Mody I (2008) Which $GABA_A$ receptor subunits are necessary for tonic inhibition in the hippocampus? J Neurosci 28:1421–1426. CrossRef Medline

Hanchar HJ, Dodson PD, Olsen RW, Otis TS, Wallner M (2005) Alcohol-induced motor impairment caused by increased extrasynaptic GABA(A) receptor activity. Nat Neurosci 8:339–345. CrossRef Medline

Hanchar HJ, Chutsrinopkun P, Meera P, Supavilai P, Sieghart W, Wallner M, Olsen RW (2006) Ethanol potently and competitively inhibits binding of the alcohol antagonist Ro15–4513 to alpha4/6beta3delta GABAA receptors. Proc Natl Acad Sci U S A 103:8546–8551. CrossRef Medline

Hyyti ä P, Koob GF (1995) GABAA receptor antagonism in the extended amygdala decreases ethanol self-administration in rats. Eur J Pharmacol 283:151–159. CrossRef Medline

Jia F, Chandra D, Homanics GE, Harrison NL (2008) Ethanol modulates synaptic and extrasynaptic GABAA receptors in the thalamus. J Pharmacol Exp Ther 326:475–482. CrossRef Medline

Jones A, Korpi ER, McKernan RM, Pelz R, Nusser Z, Mäkel ä R, Mellor JR, Pollard S, Bahn S, Stephenson FA, Randall AD, Sieghart W, Somogyi P, Smith AJ, Wisden W (1997) Ligand-gated ion channel subunit partnerships: $GABA_A$ receptor $\alpha 6$ subunit gene inactivation inhibits δ subunit expression. J Neurosci 17:1350–1362. Medline

June HL Sr, Foster KL, Eiler WJ 2nd, Goergen J, Cook JB, Johnson N, Mensah-Zoe B, Simmons JO, June HL Jr, Yin W, Cook JM, Homanics GE (2007) Dopamine and benzodiazepine-dependent mechanisms regulate the EtOH-enhanced locomotor stimulation in the GABAA alpha1 subunit null mutant mice. Neuropsychopharmacology 32 137–152. CrossRef

Justice NJ, Yuan ZF, Sawchenko PE, Vale W (2008) Type 1 corticotropin-releasing factor receptor expression reported in BAC transgenic mice: implications for reconciling ligand-receptor mismatch in the central corticotropin-releasing factor system. J Comp Neurol 511:479–496. CrossRef Medline

Koob GF (2008) A role for brain stress systems in addiction. Neuron 59:11–34. CrossRef Medline

Koob GF (2010) The role of CRF and CRF-related peptides in the dark side of addiction. Brain Res 1314:3–14. CrossRef Medline

Koob GF, Heinrichs SC (1999) A role for corticotropin releasing factor and urocortin in behavioral responses to stressors. Brain Res 848:141–152. CrossRef Medline

Krook-Magnuson EI, Huntsman MM (2005) Excitability of cortical neurons depends upon a powerful tonic conductance in inhibitory networks. Thalamus Relat Syst 3:115–120. CrossRef Medline

Liang J, Suryanarayanan A, Abriam A, Snyder B, Olsen RW, Spigelman I

(2007) Mechanisms of reversible GABAA receptor plasticity after ethanol intoxication. J Neurosci 27:12367–12377. CrossRef Medline

Liang J, Spigelman I, Olsen RW (2009) Tolerance to sedative/hypnotic actions of GABAergic drugs correlates with tolerance to potentiation of extrasynaptic tonic currents of alcohol-dependent rats. J Neurophysiol 102:224–233. CrossRef Medline

Linden AM, Schmitt U, Lepp ä E, Wulff P, Wisden W, Lüddens H, Korpi ER (2011) Ro 15–4513 antagonizes alcohol-induced sedation in mice through alphabetagamma2-type GABA(A) receptors. Front Neurosci 5:3. CrossRef Medline

Lowery-Gionta EG, Navarro M, Li C, Pleil KE, Rinker JA, Cox BR, Sprow GM, Kash TL, Thiele TE (2012) Corticotropin releasing factor signaling in the central amygdala is recruited during binge-like ethanol consumption in C57BL/6J mice. J Neurosci 32:3405–3413. CrossRef Medline

Lowery EG, Sparrow AM, Breese GR, Knapp DJ, Thiele TE (2008) The CRF-1 receptor antagonist, CP-154,526, attenuates stress-induced increases in ethanol consumption by BALB/cJ mice. Alcohol Clin Exp Res 32:240–248. CrossRef Medline

Lüddens H, Wisden W (1991) Function and pharmacology of multiple GABAA receptor subunits. Trends Pharmacol Sci 12:49–51. CrossRef Medline

Marowsky A, Rudolph U, Fritschy JM, Arand M (2012) Tonic inhibition in principal cells of the amygdala: a central role for alpha3 subunit-containing GABAA receptors. J Neurosci 32:8611–8619. CrossRef Medline

Merlo Pich E, Lorang M, Yeganeh M, Rodriguez de Fonseca F, Raber J, Koob GF, Weiss F (1995) Increase of extracellular corticotropin-releasing factor-like immunoreactivity levels in the amygdala of awake rats during restraint stress and ethanol withdrawal as measured by microdialysis. J Neurosci 15:5439–5447. Medline

Mitchell EA, Gentet LJ, Dempster J, Belelli D (2007) GABAA and glycine receptor-mediated transmission in rat lamina II neurones: relevance to the analgesic actions of neuroactive steroids. J Physiol 583:1021–1040. CrossRef Medline

Mody I, Glykys J, Wei W (2007) A new meaning for "Gin and Tonic": tonic inhibition as the target for ethanol action in the brain. Alcohol 41:145–153. CrossRef Medline

Nie Z, Schweitzer P, Roberts AJ, Madamba SG, Moore SD, Siggins GR (2004) Ethanol augments GABAergic transmission in the central amygdala via CRF1 receptors. Science 303:1512–1514. CrossRef Medline

Nie H, Rewal M, Gill TM, Ron D, Janak PH (2011) Extrasynaptic delta-containing GABAA receptors in the nucleus accumbens dorsomedial shell contribute to alcohol intake. Proc Natl Acad Sci U S A 108:4459–4464. CrossRef Medline

Pignataro L, Miller AN, Ma L, Midha S, Protiva P, Herrera DG, Harrison NL (2007) Alcohol regulates gene expression in neurons via activation of heat shock factor 1. J Neurosci 27:12957–12966. CrossRef Medline

Pirker S, Schwarzer C, Wieselthaler A, Sieghart W, Sperk G (2000) GABA(A) receptors: immunocytochemical distribution of 13 subunits in the adult rat brain. Neuroscience 101:815–850. CrossRef Medline

Roberto M, Madamba SG, Moore SD, Tallent MK, Siggins GR (2003) Ethanol increases GABAergic transmission at both pre- and postsynaptic sites in rat central amygdala neurons. Proc Natl Acad Sci U S A 100:2053–2058. CrossRef Medline

Roberto M, Madamba SG, Stouffer DG, Parsons LH, Siggins GR (2004) Increased GABA release in the central amygdala of ethanol-dependent rats. J Neurosci 24:10159–10166. CrossRef Medline

Roberto M, Cruz MT, Gilpin NW, Sabino V, Schweitzer P, Bajo M, Cottone P, Madamba SG, Stouffer DG, Zorrilla EP, Koob GF, Siggins GR, Parsons LH (2010) Corticotropin releasing factor-induced amygdala gamma-aminobutyric acid release plays a key role in alcohol dependence. Biol Psychiatry 67:831–839. CrossRef Medline

Roberts AJ, Cole M, Koob GF (1996) Intra-amygdala muscimol decreases operant ethanol self-administration in dependent rats. Alcohol Clin Exp Res 20:1289–1298. CrossRef Medline

Sakanaka M, Shibasaki T, Lederis K (1986) Distribution and efferent projections of corticotropin-releasing factor-like immunoreactivity in the rat amygdaloid complex. Brain Res 382:213–238. CrossRef Medline

Sanger DJ, Morel E, Perrault G (1996) Comparison of the pharmacological profiles of the hypnotic drugs, zaleplon and zolpidem. Eur J Pharmacol 313:35–42. CrossRef Medline

Saxena NC, Macdonald RL (1996) Properties of putative cerebellar gamma-aminobutyric acid A receptor isoforms. Mol Pharmacol 49:567–579. Medline

Scimemi A, Semyanov A, Sperk G, Kullmann DM, Walker MC (2005) Multiple and plastic receptors mediate tonic GABAA receptor currents in the hippocampus. J Neurosci 25:10016–10024. CrossRef Medline

Semyanov A, Walker MC, Kullmann DM, Silver RA (2004) Tonically active GABA A receptors: modulating gain and maintaining the tone. Trends Neurosci 27:262–269. CrossRef Medline

Stell BM, Brickley SG, Tang CY, Farrant M, Mody I (2003) Neuroactive steroids reduce neuronal excitability by selectively enhancing tonic inhibition mediated by delta subunit-containing GABAA receptors. Proc Natl Acad Sci U S A 100:14439–14444. CrossRef Medline

Sur C, Farrar SJ, Kerby J, Whiting PJ, Atack JR, McKernan RM (1999) Preferential coassembly of alpha4 and delta subunits of the gamma-aminobutyric acidA receptor in rat thalamus. Mol Pharmacol 56:110–115. Medline

Wallner M, Hanchar HJ, Olsen RW (2003) Ethanol enhances alpha 4 beta 3 delta and alpha 6 beta 3 delta gamma-aminobutyric acid type A receptors at low concentrations known to affect humans. Proc Natl Acad Sci U S A 100:15218–15223. CrossRef Medline

Wallner M, Hanchar HJ, Olsen RW (2006) Low-dose alcohol actions on alpha4beta3delta GABAA receptors are reversed by the behavioral alcohol antagonist Ro15–4513. Proc Natl Acad Sci U S A 103:8540–8545. CrossRef Medline

Wei W, Faria LC, Mody I (2004) Low ethanol concentrations selectively augment the tonic inhibition mediated by delta subunit-containing GABAA receptors in hippocampal neurons. J Neurosci 24:8379–8382. CrossRef Medline

Yang AR, Liu J, Yi HS, Warnock KT, Wang M, June HL Jr, Puche AC, Elnabawi A, Sieghart W, Aurelian L, June HL Sr (2011) Binge drinking: in search of its molecular target via the GABA(A) receptor. Front Neurosci 5:123. CrossRef Medline